CRISPR/Cas-based precision gene replacement in plants via microhomology-mediated end joining

Tien Van Vu[1,2,*], Gah-Hyun Lim[3,4], Seung Hee Choi[4], Ju Yeon Moon[4], Ngan Thi Nguyen[1], Swati Das[1], Mil Thi Tran[1], Yeon Woo Sung[1], Jihae Kim[1], Young Jong Song[1], Suk Weon Kim[4], Jae Cheol Jeong[4], Jae-Yean Kim[1,5,*]

[1]Division of Applied Life Science (BK21 FOUR Program), Plant Molecular Biology and Biotechnology Research Center, Gyeongsang National University, Jinju 660-701, Republic of Korea.

[2]National Key Laboratory for Plant Cell Biotechnology, Agricultural Genetics Institute, Km 02, Pham Van Dong Road, Co Nhue 1, Bac Tu Liem, Hanoi 11917, Vietnam.

[3]Department of Biological Sciences, Pusan National University, Busan 46241, Republic of Korea

[4]Biological Resource Center, Korea Research Institute of Bioscience and Biotechnology (KRIBB), Jeongeup, 56212, Republic of Korea

[5]Nulla Bio Inc 501 Jinju-daero, Jinju 52828, Republic of Korea.

*Correspondence: Tien Van Vu: tienvu.agi@gmail.com (ORCID: 0000-0002-6369-7664). Jae-Yean Kim: kimjy@gnu.ac.kr (ORCID ID : 0000-0002-1180-6232).

Running title: MMEJ-mediated precise gene replacement in plants.

Word count:

Main text (excluding the title page, references, figure legends, and tables): 3696/3500.

Number of Main Figures: 03

Number of Tables: 01

Number of Supplemental Figures: 06

Number of Supplemental Tables: 10

ABSTRACT

Highly efficient precision gene editing is ultimately a desirable technology, but implementation remains challenging, especially in plants. Here, we tested a novel CRISPR-Cas-based tool for precision gene replacement in plants employing a microhomology-mediated end joining (MMEJ) mechanism. The MMEJ-mediated precise gene replacement employing 20-bp microhomology MMEJ donors (~100 bp lengths) and a cNHEJ inhibitor, NU7441, produced high targeted editing efficiencies, up to 1.60 ± 0.14, 4.47 ± 1.98, and 8.98 ± 4.73 % in tomato, lettuce, and cabbage, respectively. Our data also revealed the critical impacts of the microhomology length and NU7441 concentration on MMEJ-based precision gene editing in plants.

Keywords: MMEJ, Precision gene editing, Microhomology, CRISPR/Cas, DNA repair, PITCh

INTRODUCTION

Precise modification of bases/genes of interest within their genomic context is highly desirable for gene functionalization and genetic engineering applications. However, efficient precision gene editing remains challenging in plants (Schindele et al., 2020). With the advent of the clustered regularly interspaced short palindromic repeats (CRISPR)/CRISPR-associated (Cas) technology (Jinek et al., 2012), plant precision editing has been revolutionized with homology-directed gene targeting (HGT) (Cermak et al., 2015; Vu et al., 2020; Wang et al., 2017; Wolter and Puchta, 2019; Zhang et al., 2022) and prime editing (PE) (Anzalone et al., 2020; Lin et al., 2021). With HGT, we can precisely edit genes from a single base to kilobase scales, while narrower-range precise gene editing could be achieved with the PE editing tools. However, HGT still requires improvement for practical applications to a wide range of *Arabidopsis* loci (Zhang et al., 2022) and crop plant loci due to low editing efficiency and inaccessibility of the genomic contexts of the loci (Vu et al., 2021a; Wang et al., 2017; Zhang et al., 2022). In the case of prime editors, while substantial improvements have been made to achieve efficient editing in monocots (Lin et al., 2021; Zong et al., 2022), it has not been so successful in dicot plants (Lu et al., 2020b; Vu et al., 2021b).

Double-stranded breaks (DSBs) formed by the activity of fully functional Cas9 proteins may be repaired majorly by canonical nonhomologous end-joining (cNHEJ) and homologous recombination (HR), and the former is the dominant pathway (Puchta, 2005). MMEJ, a

previously thought to be an alternative pathway of the cNHEJ, has been shown to play a more important role in DSB repair (Ata et al., 2018; Sharma et al., 2015; Tan et al., 2020). Recently, cNHEJ and MMEJ mechanisms were repurposed for CRISPR/Cas9-based precise genome editing at high efficiency and specificity in yeast and animals (Ata et al., 2018; Hayashi and Tanaka, 2019; Li et al., 2019; Sakuma et al., 2016; Yao et al., 2017). In plants, Lu and co-workers engineered a cNHEJ-mediated CRISPR/Cas9-based precise gene insertion at high efficiency by employing a single cut at genomic sites in rice (Lu et al., 2020a). However, a system exploiting cNHEJ and MMEJ for precise gene replacement has not been developed in plants.

Here, we further developed our previously proposed MMEJ-mediated precise gene editing (Vu et al., 2021c) and evaluated a novel MMEJ-based system for precise gene replacement in plants. Using PEG-mediated protoplast transfection and targeted deep sequencing methods, we successfully obtained highly precise editing efficiency in tomato, lettuce, and cabbage. The MMEJ-based precise gene replacement could be further improved by optimizing the microhomology lengths, donor template concentration, and suppression of cNHEJ by NU7441. This tool offers an alternative way for precise gene editing in plants and may help to advance crop breeding in the future.

RESULTS AND DISCUSSION

System design and validation for precise gene replacement in plants

A predefined genomic site with a protospacer adjacent motif (PAM) is determined first, thus enabling the prediction of the DSB formation site (Figure 1A and 1B). The sequence between the two predicted cut sites is employed as a donor template so that its DNA sequence is essentially modified, allowing it to carry targeted base changes to avoid recurrent cuts after gene replacement (Figure 1A, 1B, and supplemental Figure 1). In the case of MMEJ-mediated editing, the predicted flanking DSB ends would then be used to choose microhomologies (MH1, and MH2, supplemental Figure 1B) at different lengths. Still, they should be optimally at least 8 nt (up to 20 nt was reported) in size (xxxxxxxx and yyyyyyyy in Figure 1B), as suggested (Ata et al., 2018; Nakade et al., 2014; Sakuma et al., 2016).

We selected a tomato homolog of *Arabidopsis* hydroxyproline O-arabinosyltransferase 3 (SlHPAT3, accession no. Solyc07g021170) for our proof-of-concept experiments (Brooks et al.,

2014). We then employed PEG-mediated tomato protoplast transfection to deliver the SpCas9 proteins, two sgRNAs, namely gR1.HPAT3 and gR2.HPAT3 (Figure 1C) for cutting the genomic sites, and donors for replacing six base pairs of SlHPAT3 (Figure 1C; supplemental Table 1 and supplemental file 1). With the treatments of the SpCas9 protein and either of the gR1.HPAT3 or gR2.HPAT3, or both of them, without a donor, no precise edited products were found (Figure 1D). When either the NHEJ or the MMEJ donor was employed with both the gRNAs, precise replacement occurred, as shown by Sanger sequencing (supplemental Figure 2 and supplemental Table 2). Further analysis of the targeted deep-sequencing data revealed editing efficiency as high as 2.46 % (Figure 1D and supplemental Table 3) in the case of the MJ.HPAT3-1 donor. Adding the cNJ.HPAT3-1 donor also resulted in the precise replacement of some bases pre-introduced in the donor sequence at a much lower frequency of 0.09 %. Significantly, the edited products of the cNHEJ donor did not include base changes located at its two ends (supplemental Tables 2 and 3), indicating that either the donor terminal ends might be damaged before use for editing or that an unknown mechanism, possibly oligonucleotide-directed mutagenesis (ODM), might involve in the integration of the middle SNPs into the genomic sequence.

Further analysis of the edited products revealed multiple repaired products by the MJ.HPAT3-1 donor with various frequencies (Figure 1E). The precisely edited allele containing the intended base modification accounted for 9.72 % of total edited reads (supplemental Table 3). However, when we observed all the edited products containing the desirable B and C base changes and excluded the others containing one-sided base changes (A1 and A2 or D1 and D2) that were designed to prohibit the recurrent cleavages of the SpCas9, the proportion of these alleles was 33.02% of the total edited alleles (Figure 1E; supplemental Table 3). The diversity of the repaired products indicates that not only was MMEJ involved in repairing the DNA damage, but it also participated in other repair mechanisms like HR for one-sided alleles and ODM with only the B and C base changes. The initial data showed that both cNHEJ and MMEJ-mediated precision gene editing are feasible in tomatoes, with the latter performing far better than the former.

Higher donor abundance enhances HR-independent precise gene replacement

The copy number of donor DNA templates available at the targeting sites during the cleavage of CRISPR/Cas complexes was shown to be essential for enhancing HDR efficiency (Cermak et al., 2015; Vu et al., 2020; Wang et al., 2017). We sought to investigate the implications of different donor doses on the frequency of MMEJ-mediated DNA replacement. The MMEJ-mediated editing frequencies with all base changes were increased with higher amounts of donor DNA, from 10.42 % (50 pmol) to 19.84 % (300 pmol), and the one-sided repair frequencies were reduced accordingly (Figure 2A and supplemental Figure 5; supplemental Table 4). In the case of the cNJ.HPAT3-1 donor, the editing efficiency did not vary much among the donor doses and was much lower compared to that of the MJ.HPAT3-1 (Figure 2A). Again, most of its products contained only B and C changes (Supplemental Figure 5). These data indicate that the simultaneity of the MMEJ donor presence and the cleavages of the genomic sites was important for precise gene replacement since higher donor doses increased the chance of diffusing them to the being-cleaved targeted sites. The higher abundance of the donor templates might also assure sufficient amounts of undamaged donor DNA templates for editing.

The length of microhomology affects MMEJ-based precise gene replacement

The length of microhomology arms was an important parameter for activating the MMEJ pathway upon DSB formation and end resection (Villarreal et al., 2012). Effective microhomology lengths (8-20 bases) increased MMEJ-mediated gene insertion in mammalian cells (Ata et al., 2018; Nakade et al., 2014; Sakuma et al., 2016). We, therefore, tested the impact of three different microhomology lengths (20, 10, and 5 bp) on MMEJ-mediated precision editing. When the microhomology was shorter than 20 bp, the total editing efficiency was significantly reduced from 4.22 ± 0.47 % (MJ.HPAT3-1) to 2.33 ± 0.31 % (MJ.HPAT3-2) and 2.65 ± 0.58 % (MJ.HPAT3-3) (Supplemental Table 6). More importantly, the all-base-changed precise editing efficiency was significantly higher for 20-bp microhomology (0.28 ± 0.05 %) compared to that of the 10-bp (0.12 ± 0.03 %) and 5-bp (0.04 ± 0.01 %) microhomology lengths (Figure 2B). Furthermore, when we consider the reads including the B and C base changes, the targeted editing efficiency was 1.16 ± 0.09; 0.66 ± 0.12; and 0.55 ± 0.06 % for the 20-bp; 10-bp; and 5-bp microhomologies, respectively (Figure 2B; supplemental Table 6). Interestingly, the activities of the gRNAs were not significantly different among all the treatments (supplemental

Table 6), indicating that the intermolecular MMEJ-mediated editing efficiency obtained from the experiments depended on microhomology length, as shown in the cases of intramolecular MMEJ (Ata et al., 2018; Bae et al., 2014; Nakade et al., 2014). These data suggest that the 20-bp microhomology was the best among the tested lengths, confirming the highest performance of the 20-bp microhomology (Sakuma et al., 2016) for MMEJ-mediated DSB repair in plants.

NU7441 improves MMEJ-based precise gene replacement

Since the MMEJ-mediated precise editing efficiency was still low to be practically applicable for crop improvement, significant improvement of the editing system is needed. NU7441, a small chemical that was shown to inhibit DNA-dependent protein kinase (DNA-PKcs), an important cNHEJ component, enhancing HR-mediated repair of DSBs (Robert et al., 2015; Vu et al., 2021a; Zhao et al., 2006), also significantly elevated the MMEJ-mediated DSB repair products in mammalian cells (Dutta et al., 2017). We next tested if NU7441 can facilitate MMEJ repair using various concentrations of the chemical and the MJ.HPAT3-1donors. When the NU7441 concentration was increased from 0 to 1 µM, the editing efficiency was significantly elevated (Table 1 and Figure 2C). The read numbers of the precise products containing all the intended base changes, or only B and C base changes, were enhanced with the targeted editing efficiency reached up to 1.60 ± 0.14 % at 1 µM NU7441 compared to 1.03 ± 0.32 % without the addition of NU7441 (Table 1). The total editing efficiency was significantly higher with 1 µM NU7441 treatment, reaching up to 5.96 ± 0.34 %, a 1.65-fold increase compared to mock control and majorly contributed by one-side editing (Table 1) indicating that NU7441 treatment effectively favored the choice of MMEJ pathway for DSB repair. When NU7441 was added up to 2 µM, the repaired outcomes were reversely correlated with the NU7441 concentrations (Figure 2C). This result suggests that over-suppresion of the cNHEJ components might lead to cellular toxicity, as shown in mammalian cells (Robert et al., 2015), and thus negatively impact the DSB repairs (Table 1 and Figure 2C).

Taken together, MMEJ-mediated precision editing is feasible in tomatoes and might be improved by using sufficient microhomology and NU7441 treatment.

Efficient MMEJ-based precise gene replacement in lettuce and cabbage

To extend MMEJ-mediated precision gene editing to other plant species, we conducted MMEJ-mediated precise gene replacement in lettuce and cabbage using the RNP transfection method.

The *THERMO-TOLERANCE 1* (*TT1*) (Li et al., 2015), *ORANGE* (*Or*) (Yazdani et al., 2019; Yuan et al., 2015), and *ACETOLACTATE SYNTHASE 1* (*ALS1*) (Mazur et al., 1987) genes were selected as targets for both lettuce and cabbage (supplemental Figure 6). All the edited alleles of TT1, Or, and ALS1 contained a single amino acid substitution (supplemental Figure 6) for obtaining the expected traits (heat tolerance, carotenoid overaccumulation, and herbicide tolerance, respectively) (Li et al., 2015; Mazur et al., 1987; Yazdani et al., 2019; Yuan et al., 2015). Sequence alignment using tomato protein sequences was conducted using NCBI Blastp and putative TT1. Or, and ALS1 genes were subsequently identified in lettuce (supplemental Tables 7) and cabbage (supplemental Tables 8). We designed and employed two gRNAs for cutting genomic loci and MMEJ donors containing 20-base microhomologies at two ends (Figure 3A and 3B). In lettuce, the highest MMEJ-mediated precise editing efficiency for all the intended base changes was 1.81 ± 0.75 % for the *LsALS1* locus, and the lowest efficiency was zero for the *LsTT1* locus. The *LsOr* locus showed only 0.13 ± 0.10 % for the exchange of all the intended bases (Figure 3C; supplemental Table 9). As mentioned earlier, the simultaneous activity of the two gRNAs is important for MMEJ-mediated DSB repair. The data here suggest more similar cleavages between the two gRNAs of LsOr and LsALS1 compared to that of the LsTT1 (supplemental Table 9), which may partially explain the inefficiency of MMEJ-mediated repair at that locus. Considering all the repaired products that contain the targeted base changes for the desirable a.a., the efficiency reached 4.47 ± 1.98 %, 0.78 ± 0.30 %, and 0.42 ± 0.28 % for LsALS1, LsTT1, and LsOr locus, respectively (Fig 3C; supplemental Table 9).

In cabbage, the MMEJ-mediated precise gene replacement worked more efficiently than for the tomato and lettuce. The highest precise editing efficiency (7.27 ± 4.46 %) was obtained at the BoTT1 locus and lower at the BoOr gene (1.68 ± 0.24 %). The ALS1 locus for cabbage resulted in the least precise editing efficiency, at only 0.73 ± 0.43 % (Figure 3D; supplemental Table 10). Moreover, the targeted editing efficiency at the BoTT1 locus was the highest among tested loci in tomato, lettuce, and cabbage, reaching up to 8.98 ± 4.73 % (Figure 3D). In summary, the data from lettuce and cabbage indicate that MMEJ-mediated precision editing could be successfully extended to other plant species.

Notably, the MMEJ-mediated gene replacement has no limitation concerning the position and the number of base changes within the donor sequence. Such gene replacement is helpful in short sequence replacement for engineering regulatory elements, *in vivo* protein tagging, and short a.a.

modification of a protein. Multiple-site editing is also possible with the RNP-protoplast transfection, but further testing is required. This system offers another precision gene-editing tool for new plant breeding techniques that may advance crop breeding in the future.

METHODS

Donor DNA preparation for RNP works

Chemically modified donors (supplemental Table 1; supplemental file 1) were prepared by annealing of synthesized oligos or by PCRs. The 5' end modified cNJ.HPAT3-1 was prepared by PCRs using 5' modified oligos (5' phosphorylated, phosphorothioate bond addition to the phosphodiester linkage between the first and the second nucleotides) (supplemental Table 1) synthesized by Bioneer (Korea) without a template. The MMEJ donors were prepared by PCRs using complementaty oligos (supplemental Table 1) synthesized by Bioneer (Daejeon, Korea) without templates. A high-fidelity DNA Taq polymerase was used for the PCR amplifications. The PCR products were cleaned using a BIOFACT PCR cleanup kit (BIOFACT, Korea). The donor concentrations were assessed by Nanodrop2000 spectrophotometer (Thermofisher, USA) and directly used for transfection stored at -20°C for further uses.

Isolation of protoplasts

Tomato (*Solanum lycopersicum* cv. Micro-Tom*)*, lettuce (*Lactuca sativa* L. cv. Cheongchima), and cabbage (*Brassica oleracea*) seeds were sterilized with 70% ethanol for 3 min, 1% hypochlorite solution for 15 min, and washed five times with distilled water. The sterilized seeds were inoculated in a medium containing 1/2 Murashige and Skoog salts, 0.4 mg/L thiamine HCl, 100 mg/L Myo-inositol, 30 g/L sucrose, and 8 g/L gelrite, pH 5.7. The seedlings were grown in a growth chamber under a 16 h light/8 h dark photoperiod (100–130 μmol/m^2 s) at 25°C for tomato and 20°C for lettuce, and 23°C for cabbage.

For protoplast isolation of tomato and cabbage, the cotyledons of 4-day-old tomato seedlings and the cotyledons of 7-day-old cabbage seedlings were immersed in cell and protoplast washing solution (CPW) containing 0.5% cellulase (Novozymes, Basgsvaerd, Denmark), 0.5% pectinase (Novozymes, Bagsværd, Denmark), 1% viscozyme (Novozymes, Bagsværd, Denmark), 3 mM MES (pH 5.8) and 9% mannitol. After 15 min of vacuum infiltration, the suspension was incubated for 2-4 hr on a rotary shaker at 50 rpm at 25°C. The suspension was filtered through an eight-layer

gauze and centrifuged for 5 min at 100 *g*. Protoplasts were separated on a 21% sucrose density gradient and then collected at the interface of the W5 solution (2 mM MES pH 5.8, 154 mM NaCl, 125 mM $CaCl_2$, 5 mM KCl). The harvested protoplasts were washed three times with W5 solution and then resuspended in MMG solution (4 mM MES pH 5.7, 0.4 M mannitol, 15 mM $MgCl_2$). The concentration of protoplasts was determined using a hemocytometer.

For the lettuce protoplast isolation, the cotyledons of 7 d-old seedlings were digested with 10 mL of enzyme solution (1% [w/v] Viscozyme (Novozymes, Bagsværd, Denmark), 0.5% Celluclast (Novozymes, Bagsværd, Denmark), and 0.5% Pectinex (Novozymes, Bagsværd, Denmark), 3 mM MES (2-[N-Morpholino] ethanesulfonic acid), pH 5.7 and 9% mannitol in CPW salts with shaking at 40 rpm for 4–6 h at 25 °C in the dark. The protoplast mixture was then filtered through a 40 µm nylon cell strainer and collected by centrifugation at 800 rpm for 5 min in a 14 mL round tube. The collected protoplasts were re-suspended in W5 solution (2 mM MES [pH 5.7], 154 mM NaCl, 125 mM $CaCl_2$, and 5 mM KCl) and further centrifuged at 800 rpm for 5 min. Finally, the protoplasts were re-suspended in W5 solution and counted under a microscope using a hemocytometer. Protoplasts were adjusted to a 1 × 106/mL density in MMG solution before transfection. The transfected protoplasts were cultured in protoplast culture medium (MS medium containing 0.4 mg/L thiamine HCl, 100 mg/L Myo-inositol, 30 g/L sucrose, 0.2 mg/L 2,4-dichlorophenoxyacetic acid [2,4-D], and 0.3 mg/L 6-benzylaminopurine [BAP], pH 5.7) in the dark f at 25°C for 4 weeks.

PEG-mediated RNP and donor transfections

SpCas9 protein was purchased from ToolGen, Inc. (Seoul, South Korea), and guide RNAs were synthesized by GeneArt Precision gRNA Synthesis Kit (Invitrogen, Massachusetts, USA) according to the manufacturer's protocol. PEG-mediated RNP and donor transfections were performed in the previous study (Woo et al., 2015).

For ribonucleoprotein (RNP) and donor DNA transfections with tomato and cabbage protoplasts, 2×10^5 protoplasts were transfected with the purified SpCas9 protein (20 µg) premixed with sgRNAs (10 µg each) and donor templates in PBS buffer followed by incubating for 10 min at 25°C. The RNP complexes were mixed with protoplasts and then supplemented with an equal volume of 40% PEG transfection solution (40% PEG 4000, 0.2 M mannitol, and 0.1 M $CaCl_2$). This suspension was mixed gently and then incubated at room temperature for 10 min. An equal

volume of W5 solution was added for washing, followed by centrifugation at 100 *g* for 5 min. The supernatant was discarded, and the protoplasts were incubated with 1 ml of W5 solution in the dark at 25°C for 48 h. Afterward, the cells were collected for gDNA isolation and subsequent targeted deep sequencing analysis.

For lettuce protoplast transfection, SpCas9 protein and sgRNAs were premixed in 1× NEB buffer 3 for at least 10 minutes at room temperature, and 2×10^5 protoplast cells were transfected with SpCas9 protein (20 μg) premixed with sgRNAs (10 μg each) and donor DNA. A mixture of 2×10^5 protoplast cells was re-suspended in 200 μl MMG solution and then was slowly mixed with RNP complex, donor, and 350 μl of PEG solution (40% [w/v] PEG 4000, 0.2 M mannitol, and 0.1 M CaCl2). After incubation for 10 min, the transfected protoplast cells were gently re-suspended in 650 μL W5 solution. After additional incubation for 10 min, 650 μL W5 solution was added slowly again and was mixed well by inverting the tube. Protoplasts were pelleted by centrifugation at 556 rpm for 5 min and washed gently in 1 ml W5 solution. Protoplasts were pelleted by centrifugation at 556 rpm for 5 min and re-suspended gently in 1 ml WI solution (4 mM MES [pH 5.7], 0.5 M mannitol, and 20 mM KCl). Finally, the protoplasts were transferred into a 60 × 15 mm petri dish (Falcon), cultured under dark conditions at 25°C for 48 h, and then analyzed for genome editing efficiency.

Targeted deep sequencing

Genomic DNAs were isolated from the protoplasts using the CTAB method. We used the miniseq sequencing service (MiniSeqTM System, Illumina, USA) to obtain targeted deep sequencing of the edited genomic sites. Miniseq samples were prepared in three PCRs according to the manufacturer’s guidelines, with genomic DNAs as the first PCR template. The first and second PCRs used primers listed in supplemental Table 1, whereas the third PCRs were conducted with the manufacturer's primers to assign a sample ID. A high-fidelity DNA Taq polymerase (Phusion, NEB, USA) was used for the PCRs. The miniseq raw data FASTQ files were analyzed using the Cas-Analyzer tool (Park et al., 2016). The indel examining window was set at 5 bases with a comparison range that covered both the read ends. A similar analysis was conducted for the targeted base changes of lettuce and cabbage genes.

Statistical analysis

The editing data, statistical analysis, and plots were further processed by the MS Excel and Graphpad Prism 9.0 programs and are explained in detail in the legends of figures and tables wherever applicable.

FUNDING

This work was supported by the National Research Foundation of Korea (Grant NRF 2020R1I1A1A01072130, 2020M3A9I4038352, 2020R1A6A1A03044344, 2021R1A5A8029490, 2022R1A2C3010331) and the Program for New Plant Breeding Techniques (NBT, Grant PJ01478401), Rural Development Administration (RDA), Korea.

AUTHOR CONTRIBUTIONS

Conceptualization, T.V. V and J.Y.K.; Methodology, T.V. V and J.Y.K.; Conducted experiments, T.V. V., G.H.L, S.H.C, J.Y.M., S.W.K., J.C.J, N.T.N, S.D., M.T.T., Y.W.S, J.K, Y.J.S; Data analysis, T.V. V. and J.Y.K.; Writing – Original Draft, T.V. V.; Writing – Review & Editing, T.V. V. and J.Y.K.; Funding Acquisition, T.V.V., and J.Y.K.; and Supervision, T.V. V and J.Y.K.

ACKNOWLEDGEMENTS

The authors have applied for Korean patents (10-2021-0089814) and PCT patents (PCT-KR2021-008727) based on the results reported in this paper.

REFERENCES

Anzalone, A.V., Koblan, L.W., and Liu, D.R. (2020). Genome editing with CRISPR-Cas nucleases, base editors, transposases and prime editors. Nat Biotechnol *38*, 824-844.

Ata, H., Ekstrom, T.L., Martinez-Galvez, G., Mann, C.M., Dvornikov, A.V., Schaefbauer, K.J., Ma, A.C., Dobbs, D., Clark, K.J., and Ekker, S.C. (2018). Robust activation of microhomology-mediated end joining for precision gene editing applications. PLoS Genet *14*, e1007652.

Bae, S., Kweon, J., Kim, H.S., and Kim, J.S. (2014). Microhomology-based choice of Cas9 nuclease target sites. Nat Methods *11*, 705-706.

Brooks, C., Nekrasov, V., Lippman, Z.B., and Van Eck, J. (2014). Efficient gene editing in tomato in the first generation using the clustered regularly interspaced short palindromic repeats/CRISPR-associated9 system. Plant Physiol *166*, 1292-1297.

Cermak, T., Baltes, N.J., Cegan, R., Zhang, Y., and Voytas, D.F. (2015). High-frequency, precise modification of the tomato genome. Genome Biol *16*, 232.

Dutta, A., Eckelmann, B., Adhikari, S., Ahmed, K.M., Sengupta, S., Pandey, A., Hegde, P.M., Tsai, M.S., Tainer, J.A., Weinfeld, M., *et al.* (2017). Microhomology-mediated end joining is

activated in irradiated human cells due to phosphorylation-dependent formation of the XRCC1 repair complex. Nucleic Acids Res *45*, 2585-2599.
Hayashi, A., and Tanaka, K. (2019). Short-Homology-Mediated CRISPR/Cas9-Based Method for Genome Editing in Fission Yeast. G3 (Bethesda) *9*, 1153-1163.
Jinek, M., Chylinski, K., Fonfara, I., Hauer, M., Doudna, J.A., and Charpentier, E. (2012). A programmable dual-RNA-guided DNA endonuclease in adaptive bacterial immunity. Science *337*, 816-821.
Li, P., Zhang, L., Li, Z., Xu, C., Du, X., and Wu, S. (2019). Cas12a mediates efficient and precise endogenous gene tagging via MITI: microhomology-dependent targeted integrations. Cell Mol Life Sci.
Li, X.M., Chao, D.Y., Wu, Y., Huang, X., Chen, K., Cui, L.G., Su, L., Ye, W.W., Chen, H., Chen, H.C., *et al.* (2015). Natural alleles of a proteasome alpha2 subunit gene contribute to thermotolerance and adaptation of African rice. Nat Genet *47*, 827-833.
Lin, Q., Jin, S., Zong, Y., Yu, H., Zhu, Z., Liu, G., Kou, L., Wang, Y., Qiu, J.-L., Li, J., *et al.* (2021). High-efficiency prime editing with optimized, paired pegRNAs in plants. Nature Biotechnology *39*, 923-927.
Lu, Y., Tian, Y., Shen, R., Yao, Q., Wang, M., Chen, M., Dong, J., Zhang, T., Li, F., Lei, M., *et al.* (2020a). Targeted, efficient sequence insertion and replacement in rice. Nat Biotechnol *38*, 1402-1407.
Lu, Y., Tian, Y., Shen, R., Yao, Q., Zhong, D., Zhang, X., and Zhu, J.K. (2020b). Precise genome modification in tomato using an improved prime editing system. Plant Biotechnol J.
Mazur, B.J., Chui, C.F., and Smith, J.K. (1987). Isolation and characterization of plant genes coding for acetolactate synthase, the target enzyme for two classes of herbicides. Plant Physiol *85*, 1110-1117.
Nakade, S., Tsubota, T., Sakane, Y., Kume, S., Sakamoto, N., Obara, M., Daimon, T., Sezutsu, H., Yamamoto, T., Sakuma, T., *et al.* (2014). Microhomology-mediated end-joining-dependent integration of donor DNA in cells and animals using TALENs and CRISPR/Cas9. Nat Commun *5*, 5560.
Park, J., Lim, K., Kim, J.-S., and Bae, S. (2016). Cas-analyzer: an online tool for assessing genome editing results using NGS data. Bioinformatics *33*, 286-288.
Puchta, H. (2005). The repair of double-strand breaks in plants: mechanisms and consequences for genome evolution. J Exp Bot *56*, 1-14.
Robert, F., Barbeau, M., Ethier, S., Dostie, J., and Pelletier, J. (2015). Pharmacological inhibition of DNA-PK stimulates Cas9-mediated genome editing. Genome Med *7*, 93.
Sakuma, T., Nakade, S., Sakane, Y., Suzuki, K.T., and Yamamoto, T. (2016). MMEJ-assisted gene knock-in using TALENs and CRISPR-Cas9 with the PITCh systems. Nat Protoc *11*, 118-133.
Schindele, A., Dorn, A., and Puchta, H. (2020). CRISPR/Cas brings plant biology and breeding into the fast lane. Curr Opin Biotechnol *61*, 7-14.
Sharma, S., Javadekar, S.M., Pandey, M., Srivastava, M., Kumari, R., and Raghavan, S.C. (2015). Homology and enzymatic requirements of microhomology-dependent alternative end joining. Cell Death Dis *6*, e1697.
Tan, J., Zhao, Y., Wang, B., Hao, Y., Wang, Y., Li, Y., Luo, W., Zong, W., Li, G., Chen, S., *et al.* (2020). Efficient CRISPR/Cas9-based plant genomic fragment deletions by microhomology-mediated end joining. Plant Biotechnol J.

Villarreal, D.D., Lee, K., Deem, A., Shim, E.Y., Malkova, A., and Lee, S.E. (2012). Microhomology directs diverse DNA break repair pathways and chromosomal translocations. PLoS Genet *8*, e1003026.

Vu, T.V., Doan, D.T.H., Tran, M.T., Sung, Y.W., Song, Y.J., and Kim, J.-Y. (2021a). Improvement of the LbCas12a-crRNA System for Efficient Gene Targeting in Tomato. *12*.

Vu, T.V., Kim, J., Das, S., Lee, J., and Kim, J.-Y. (2021b). The obstacles and potential clues of prime editing applications in tomato, a dicot plant. 2021.2003.2015.435378.

Vu, T.V., Sivankalyani, V., Kim, E.-J., Doan, D.T.H., Tran, M.T., Kim, J., Sung, Y.W., Park, M., Kang, Y.J., and Kim, J.-Y. (2020). Highly efficient homology-directed repair using CRISPR/Cpf1-geminiviral replicon in tomato. Plant Biotechnology Journal *18*, 2133-2143.

Vu, T.V., Thi Hai Doan, D., Kim, J., Sung, Y.W., Thi Tran, M., Song, Y.J., Das, S., and Kim, J.-Y. (2021c). CRISPR/Cas-based precision genome editing via microhomology-mediated end joining. Plant Biotechnology Journal *19*, 230-239.

Wang, M., Lu, Y., Botella, J.R., Mao, Y., Hua, K., and Zhu, J.K. (2017). Gene Targeting by Homology-Directed Repair in Rice Using a Geminivirus-Based CRISPR/Cas9 System. Mol Plant *10*, 1007-1010.

Wolter, F., and Puchta, H. (2019). In planta gene targeting can be enhanced by the use of CRISPR/Cas12a. The Plant Journal *100*, 1083-1094.

Woo, J.W., Kim, J., Kwon, S.I., Corvalan, C., Cho, S.W., Kim, H., Kim, S.G., Kim, S.T., Choe, S., and Kim, J.S. (2015). DNA-free genome editing in plants with preassembled CRISPR-Cas9 ribonucleoproteins. Nat Biotechnol *33*, 1162-1164.

Yao, X., Wang, X., Liu, J., Hu, X., Shi, L., Shen, X., Ying, W., Sun, X., Wang, X., Huang, P., *et al.* (2017). CRISPR/Cas9 - Mediated Precise Targeted Integration In Vivo Using a Double Cut Donor with Short Homology Arms. EBioMedicine *20*, 19-26.

Yazdani, M., Sun, Z., Yuan, H., Zeng, S., Thannhauser, T.W., Vrebalov, J., Ma, Q., Xu, Y., Fei, Z., Van Eck, J., *et al.* (2019). Ectopic expression of ORANGE promotes carotenoid accumulation and fruit development in tomato. Plant Biotechnol J *17*, 33-49.

Yuan, H., Owsiany, K., Sheeja, T.E., Zhou, X., Rodriguez, C., Li, Y., Welsch, R., Chayut, N., Yang, Y., Thannhauser, T.W., *et al.* (2015). A Single Amino Acid Substitution in an ORANGE Protein Promotes Carotenoid Overaccumulation in Arabidopsis. Plant Physiol *169*, 421-431.

Zhang, Z., Zeng, W., Zhang, W., Li, J., Kong, D., Zhang, L., Wang, R., Peng, F., Kong, Z., Ke, Y., *et al.* (2022). Insights into the molecular mechanisms of CRISPR/Cas9-mediated gene targeting at multiple loci in Arabidopsis. Plant Physiology, kiac431.

Zhao, Y., Thomas, H.D., Batey, M.A., Cowell, I.G., Richardson, C.J., Griffin, R.J., Calvert, A.H., Newell, D.R., Smith, G.C., and Curtin, N.J. (2006). Preclinical evaluation of a potent novel DNA-dependent protein kinase inhibitor NU7441. Cancer Res *66*, 5354-5362.

Zong, Y., Liu, Y., Xue, C., Li, B., Li, X., Wang, Y., Li, J., Liu, G., Huang, X., Cao, X., *et al.* (2022). An engineered prime editor with enhanced editing efficiency in plants. Nature Biotechnology *40*, 1394-1402.

FIGURE LEGEND

Figure 1. HR-independent precision editing approaches using CRISPR/SpCas9.

(**A**) Model of sequence design for cNHEJ-based precise gene replacement.

(**B**) Model of sequence design for MMEJ-bases precise gene replacement. The cut sites are arranged to avoid recurrent cutting. Active PAM sites are shown in purple. Guide RNA sequences or traces of them in repaired products are underlined. The red xxxxxxxx represents MH1, whereas the green yyyyyyyy represents MH2. The orange sequences denote donors, and the gray indicates the genomic sequence being replaced. The red asterisks represent sequence modifications of interest. The letters n, x, and y represent any nucleotide of A, T, G, or C, except that the sequence-making gRNA spacers should not have more than 4 T in a row to avoid early transcription termination. To prevent the recurrent cut, the PAM sequence corresponding to the replaced genomic sequence should be changed. Usually, nGG/CCn is changed to nHG/CDn where H=A or C or T; D=A or G or T. One or some bases within the core spacer sequence (i.e., ~12 base-pairs upstream/downstream of nGG/CCn) could also be changed. Such changes should not lead to changes in protein sequences of the targeted gene.

(**C**) Schematic diagrams of cNHEJ- and MMEJ-mediated gene editing of tomato targeted loci SlHPAT3 (with their GenBank accession number), targeted sequences, gRNA binding sites, and donor sense sequences (cNJ.HPAT3-1, MJ.HPAT3-1, MJ.HPAT3-2, and MJ.HPAT3-3). The targeted genes are shown from the start codon (ATG) to the stop codon (TAA), exons are drawn as blue boxes, and the discontinuous lines in each gene represent intron parts of the gene; the gRNA binding sequences at the genomic locus are highlighted in light blue color and arrows with PAMs (bold nucleotides). The expected cutting sites (3-nt upstream of a PAM) are indicated with the black scissors; the intended base changes are painted in the red font that is denoted by the discontinuous red boxes and named as A1, A2, B, C, D1, and D2 on the top of the boxes. The cNHEJ donor dsDNA is synthesized with 5’-phosphorylated-ends, and the phosphodiester bonds between the first and the second nucleotides of 5’ ends were chemically modified with phosphorothioate linkages. The two red, discontinuous crossing lines indicate the MMEJ-mediated replacement sites of the MJ.HPAT3-1 donor. For the donors with shorter microhomology, the recombination lengths reduce accordingly. The diagrams are not drawn to their scales.

(**D**) cNHEJ and MMEJ-mediated editing efficiency at the SlHPAT3 locus. The editing efficiency is calculated by dividing the total reads containing the intended bases by the total reads without considering the indel mutation efficiency of the gRNAs.

(**E**) Editing frequency of respective repaired products/alleles revealed from miniseq data. The edited base-changed sets/alleles revealed from miniseq data are classified according to the presence of the base changes in the edited reads. A total of 11 base-changed sets/alleles are recorded and plotted with their relative frequency among all the edited reads.

Figure 2. Optimization of MMEJ-mediated precision gene editing in tomato.

(A) Editing efficiency revealed from targeted deep sequencing data of the various donor doses.

(B) Editing efficiencies revealed from the treatments of donors with different microhomology lengths. Targeted deep sequencing data were collected in four replicates with no donor (-donor, Mock) control.

(C) Editing efficiency revealed from targeted deep sequencing data of the treatments at different NU7441 concentrations. Targeted deep sequencing data were collected in three replicates.

The data in (**B**) and (**C**) were analyzed by the Cas-Analyzer tool, statistically analyzed (multiple comparisons used Uncorrected Fisher's LSD test) and plotted by Graphpad Prism 9. The p values are shown on the top of each compared pair. Targeted-editing efficiency is the sum of the precise editing efficiency and the only B and C editing efficiency. Precise editing efficiency was calculated by dividing total reads containing all the base changes by the total reads. The only B and C editing efficiency was calculated by dividing total reads containing only B and C base changes by the total reads. One-sided editing efficiency was calculated by dividing total reads containing only either the left-sided bases (A1 and A2) or the right-sided base pairs (D1 and D2) by the total reads.

Figure 3. MMEJ-mediated precision gene editing in lettuce and cabbage.

(A-B) Schematic diagrams of targeted loci (TT1, Or, and ALS1 with their GenBank accession number), targeted sequences, gRNA binding sites, and MMEJ donors in lettuce (**A**) and cabbage (**B**). The targeted genes are shown from the start codon (ATG) to stop codons. Exons are drawn as colored boxes (purple boxes with lettuce's loci and pink boxes for cabbage), and the discontinuous line in each gene represents intron parts of the gene; the gRNA binding sequences are highlighted in light blue color with PAMs (bold nucleotides). The expected cutting sites (3-nt upstream of a PAM) are indicated with the black scissors; the intended base changes are painted in the red font; the targeted amino acid changes and corresponding triplexes are denoted by the

discontinuous red boxes, and the texts placed on their top. The diagrams are not drawn to their scales.

(**C**) MMEJ-mediated editing efficiency in lettuce at the TT1, Or, and ALS1 loci.

(**D**) MMEJ-mediated editing efficiency in cabbage at the TT1, Or, and ALS1 loci.

TABLES

Table 1. The detailed targeted deep sequencing data revealed from the various NU7441 concentrations

SUPPLEMENTAL ITEM

Supplemental figure legends

Supplemental Figure 1. HR-independent strategies for precision gene/allele replacement using CRISPR/SpCas9

Supplemental Figure 2. Sanger sequencing data revealed precise replacement of DNA by MMEJ donor

Supplemental Figure 3. Indel alleles revealed from transfection of SpCas9, gR1.HPAT1 and gR2.HPAT3 with cNJ.HPAT3-1 donor

Supplemental Figure 4. Indel alleles revealed from transfection of SpCas9, gR1.HPAT1 and gR2.HPAT3 with MJ.HPAT3-1 donor

Supplemental Figure 5. The frequency of the MMEJ-mediated repaired products at different donor doses

Supplemental Figure 6. Identification of TT1, Or, and ALS1 genes in lettuce and cabbage for MMEJ-mediated gene targeting

Supplemental Tables

Supplemental Table 1. gRNA, donor, and primer sequences employed in the study

Supplemental Table 2. cNHEJ- and MMEJ-mediated editing rates at SlHPAT3 locus revealed by Sanger sequencing

Supplemental Table 3. cNHEJ- and MMEJ-mediated editing rates of various repaired products at SlHPAT3 locus

Supplemental Table 4. Editing frequency of various repaired products revealed from treatments of different donor types and doses

Supplemental Table 5. MMEJ-mediated gene editing using various MJ.HPAT3-1 donor amounts (replicate)

Supplemental Table 6. MMEJ-mediated editing efficiency revealed from DSBs repair using donors with different microhomology lengths.

Supplemental Table 7. Sequence alignment for selection of targeted genes in lettuce

Supplemental Table 8. Sequence alignment for selection of targeted genes in cabbage

Supplemental Table 9. Data revealed from the targeted deep-sequencing analysis of MMEJ-mediated editing in lettuce

Supplemental Table 10. Data revealed from the targeted deep-sequencing analysis of MMEJ-mediated editing in cabbage

Supplemental files

Supplemental file 1: Sequences used in the study

Table 1. The detailed targeted deep sequencing data revealed from the various NU7441 concentrations

Treatment	Replicate	NU7441 (uM)	Total reads	Total editing efficiency (%)	Precise editing efficiency (%)[a]	Targeted editing efficiency (%)[b]	Only B-C editing efficiency (%)[c]	One-sided editing efficiency (%)[d]	gRNA1 indel rate (%)	gRNA2 indel rate (%)
NU0	1	0.0	22605	3.67	0.23	0.86	0.63	2.81	3.36	4.20
	2	0.0	29443	2.18	0.09	0.58	0.49	1.59	3.05	2.97
	3	0.0	88974	4.97	0.32	1.65	1.33	3.32	0.58	0.69
Average			-	3.60	0.21	1.03	0.82	2.57	2.33	2.62
SEM			-	0.81	0.07	0.32	0.26	0.51	0.88	1.03
NU0.5	1	0.5	23931	5.39	0.24	1.35	1.11	4.04	4.76	4.71
	2	0.5	22605	4.14	0.23	1.13	0.91	3.00	3.36	3.40
	3	0.5	78738	5.70	0.42	1.86	1.44	3.84	0.53	0.55
Average			-	5.08	0.29	1.45	1.15	3.63	2.88	2.89
SEM			-	0.48	0.06	0.22	0.16	0.32	1.24	1.23
p-value (compared to NU0)				0.0740	0.0387	0.2280	0.2157	0.0544	0.7459	0.8778
NU1	1	1.0	28953	6.55	0.32	1.69	1.36	4.86	3.94	4.02
	2	1.0	30859	5.38	0.30	1.33	1.02	4.06	4.25	4.21
	3	1.0	79749	5.94	0.37	1.79	1.42	4.15	0.82	0.82
Average			-	5.96	0.33	1.60	1.27	4.35	3.00	3.02
SEM			-	0.34	0.02	0.14	0.13	0.25	1.10	1.10
p-value (compared to NU0)				0.0111	0.1666	0.1102	0.1101	0.0051	0.6938	0.8192
NU2	1	2.0	25789	3.95	0.13	0.90	0.76	3.05	3.63	3.70
	2	2.0	29652	4.44	0.24	1.14	0.90	3.30	6.03	5.91
	3	2.0	80326	4.53	0.32	1.54	1.22	3.00	1.23	1.18
Average			-	4.31	0.23	1.19	0.96	3.12	3.63	3.59
SEM			-	0.18	0.05	0.19	0.13	0.09	1.39	1.36
p-value (compared to NU0)				0.3565	0.8333	0.6226	0.5828	0.2789	0.4533	0.5769

a, Precise editing efficiency was calculated by dividing total reads containing all the base changes by the total reads. b, Targeted editing efficiency is the sum of precise editing efficiency and only B and C editing efficiency. c, The only B and C editing efficiency was calculated by dividing total reads containing only B and C base changes by the total reads. d, One-sided editing efficiency was calculated by dividing total reads containing only either the left-sided bases (A1 and A2) or the right-sided base pairs (D1 and D2) by the total reads. The total editing efficiency is the sum of the MMEJ-mediated editing efficiency (a+b+c+d).

Figure 1

A

Donor 5’ nnnnHGnnnnnnnnnnnnnn*…*nnnnnnnnnnnnnnnDCnnn 3’

Genomic locus 5’…nnnnnnnnnnnnnnnnnnnnnnnnGGnnn…nnnCCnnnnnnnnnnnnnnnnnnnnnnnnn…3’

cNHEJ repaired genomic locus 5’…nnnnnnnnnnnnnnnnHGnnnnnnnnnnnnnn*…*nnnnnnnnnnnnnnnDCnnnnnnnnnnnnn…3’

B

Donor 5’ xxxxxxxxnnnnHGnnnnnn*…*nnnnnnnDCnnnyyyyyyyy 3’

Genomic locus 5’…nnnnnnnnnnnnnxxxxxxxxnnnnGGnnn…nnnCCnnnnyyyyyyyynnnnnnnnnnn…3’

MMEJ repaired genomic locus 5’…nnnnnnnnnnnnnxxxxxxxxnnnnHGnnnnnn*…*nnnnnnnDCnnnyyyyyyyynnnnnnnnnnn…3’

C

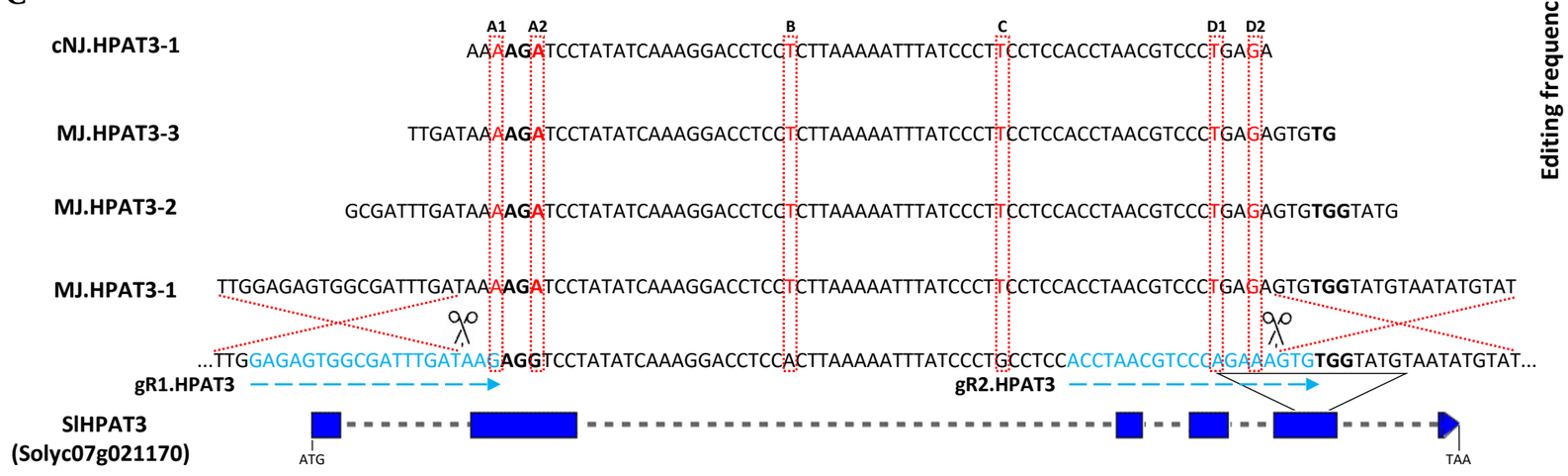

D

Treatment	SpCas9	gR1.HPAT3	gR2.HPAT3	Donor	Total reads	Editing efficiency (%)
1	-	-	-	-	121368	0.00
2	+	+	-	-	110285	0.00
3	+	-	+	-	105799	0.00
4	+	+	+	-	117136	0.00
5	+	+	+	cNJ.HPAT3-1	93054	0.09
6	+	+	+	MJ.HPAT3 -1	99885	2.46

E

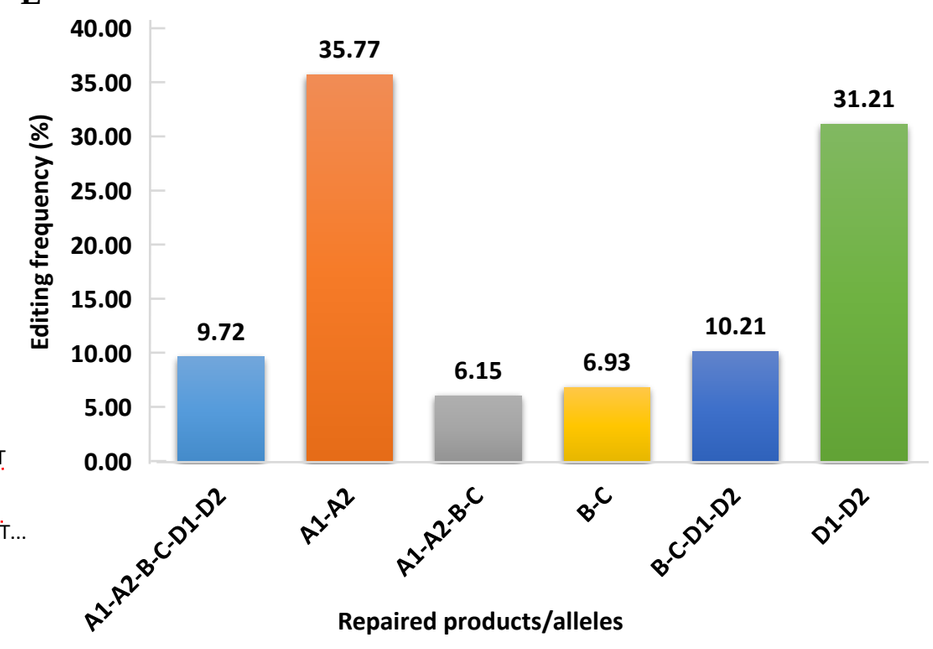

Figure 1. HR-independent precision editing approaches using CRISPR/SpCas9.

(A) Model of sequence design for cNHEJ-based precise gene replacement.

(B) Model of sequence design for MMEJ-bases precise gene replacement. The cut sites are arranged to avoid recurrent cutting. Active PAM sites are shown in purple. Guide RNA sequences or traces of them in repaired products are underlined. The red xxxxxxxx represents MH1, whereas the green yyyyyyyy represents MH2. The orange sequences denote donors, and the gray indicates the genomic sequence being replaced. The red asterisks represent sequence modifications of interest. The letters n, x, and y represent any nucleotide of A, T, G, or C, except that the sequence-making gRNA spacers should not have more than 4 T in a row to avoid early transcription termination. To prevent the recurrent cut, the PAM sequence corresponding to the replaced genomic sequence should be changed. Usually, nGG/CCn is changed to nHG/CDn where H=A or C or T; D=A or G or T. One or some bases within the core spacer sequence (i.e., ~12 base-pairs upstream/downstream of nGG/CCn) could also be changed. Such changes should not lead to changes in protein sequences of the targeted gene.

(C) Schematic diagrams of cNHEJ- and MMEJ-mediated gene editing of tomato targeted loci SlHPAT3 (with their GenBank accession number), targeted sequences, gRNA binding sites, and donor sense sequences (cNJ.HPAT3-1, MJ.HPAT3-1, MJ.HPAT3-2, and MJ.HPAT3-3). The targeted genes are shown from the start codon (ATG) to the stop codon (TAA), exons are drawn as blue boxes, and the discontinuous lines in each gene represent intron parts of the gene; the gRNA binding sequences at the genomic locus are highlighted in light blue color and arrows with PAMs (bold nucleotides). The expected cutting sites (3-nt upstream of a PAM) are indicated with the black scissors; the intended base changes are painted in the red font that is denoted by the discontinuous red boxes and named as A1, A2, B, C, D1, and D2 on the top of the boxes. The cNHEJ donor dsDNA is synthesized with 5'-phosphorylated-ends, and the phosphodiester bonds between the first and the second nucleotides of 5' ends were chemically modified with phosphorothioate linkages. The two red, discontinuous crossing lines indicate the MMEJ-mediated replacement sites of the MJ.HPAT3-1 donor. For the donors with shorter microhomology, the recombination lengths reduce accordingly. The diagrams are not drawn to their scales.

(D) cNHEJ and MMEJ-mediated editing efficiency at the SlHPAT3 locus. The editing efficiency is calculated by dividing the total reads containing the intended bases by the total reads without considering the indel mutation efficiency of the gRNAs.

(E) Editing frequency of respective repaired products/alleles revealed from miniseq data. The edited base-changed sets/alleles revealed from miniseq data are classified according to the presence of the base changes in the edited reads. A total of 11 base-changed sets/alleles are recorded and plotted with their relative frequency among all the edited reads.

Figure 2

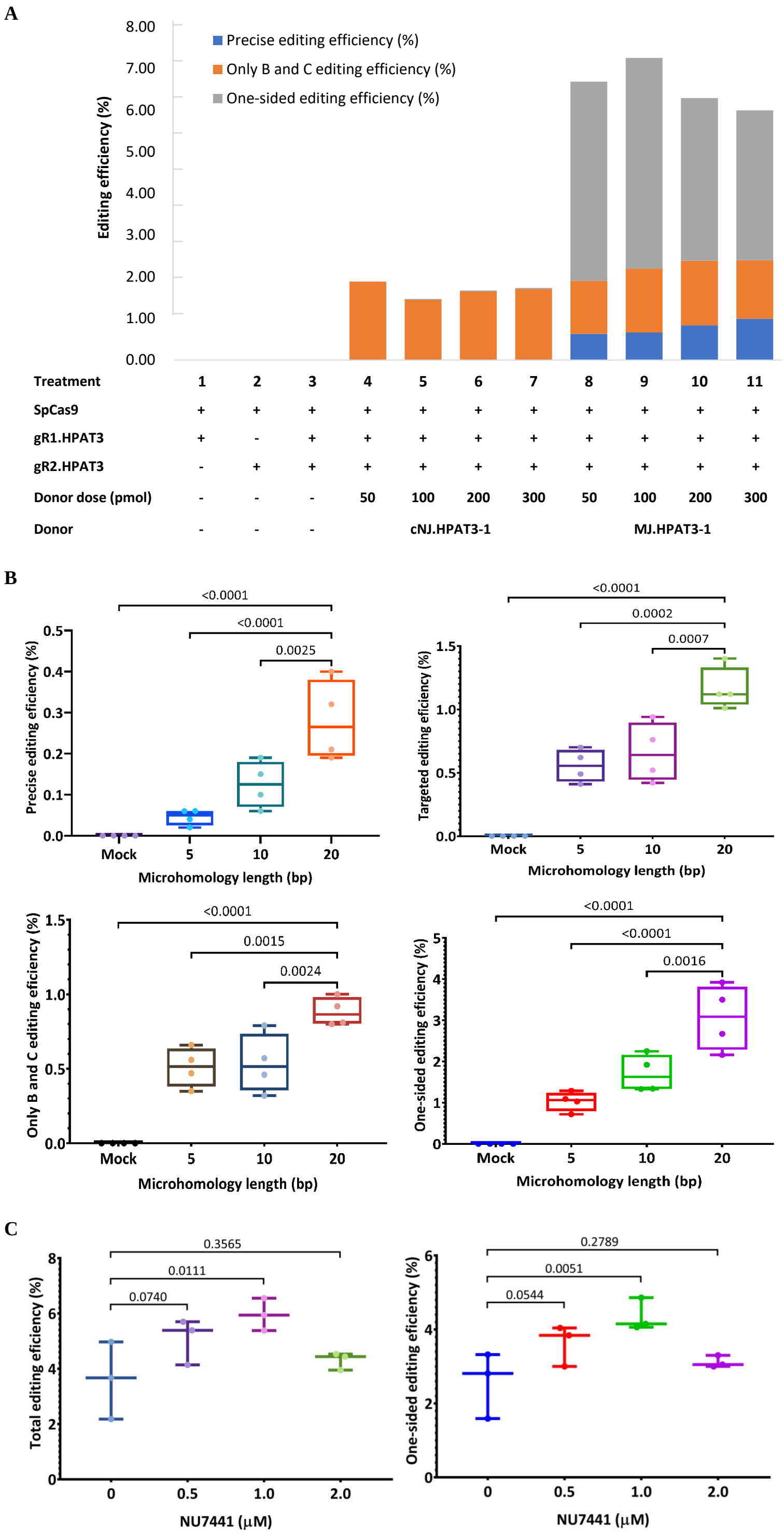

Figure 2. Optimization of MMEJ-mediated precision gene editing in tomato.

(A) Editing efficiency revealed from targeted deep sequencing data of the various donor doses.

(B) Editing efficiencies revealed from the treatments of donors with different microhomology lengths. Targeted deep sequencing data were collected in four replicates with no donor (-donor, Mock) control.

(C) Editing efficiency revealed from targeted deep sequencing data of the treatments at different NU7441 concentrations. Targeted deep sequencing data were collected in three replicates.

The data in (**B**) and (**C**) were analyzed by the Cas-Analyzer tool, statistically analyzed (multiple comparisons used Uncorrected Fisher's LSD test) and plotted by Graphpad Prism 9. The p values are shown on the top of each compared pair. Targeted editing efficiency is the sum of the precise editing efficiency and the only B and C editing efficiency. Precise editing efficiency was calculated by dividing total reads containing all the base changes by the total reads. The only B and C editing efficiency was calculated by dividing total reads containing only B and C base changes by the total reads. One-sided editing efficiency was calculated by dividing total reads containing only either the left-sided bases (A1 and A2) or the right-sided base pairs (D1 and D2) by the total reads.

Figure 3

A

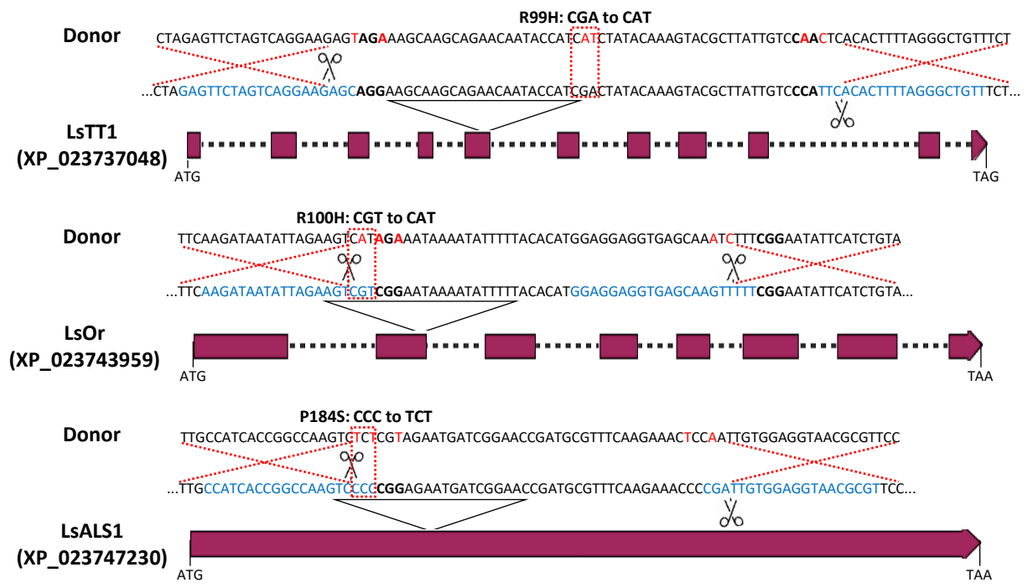

B

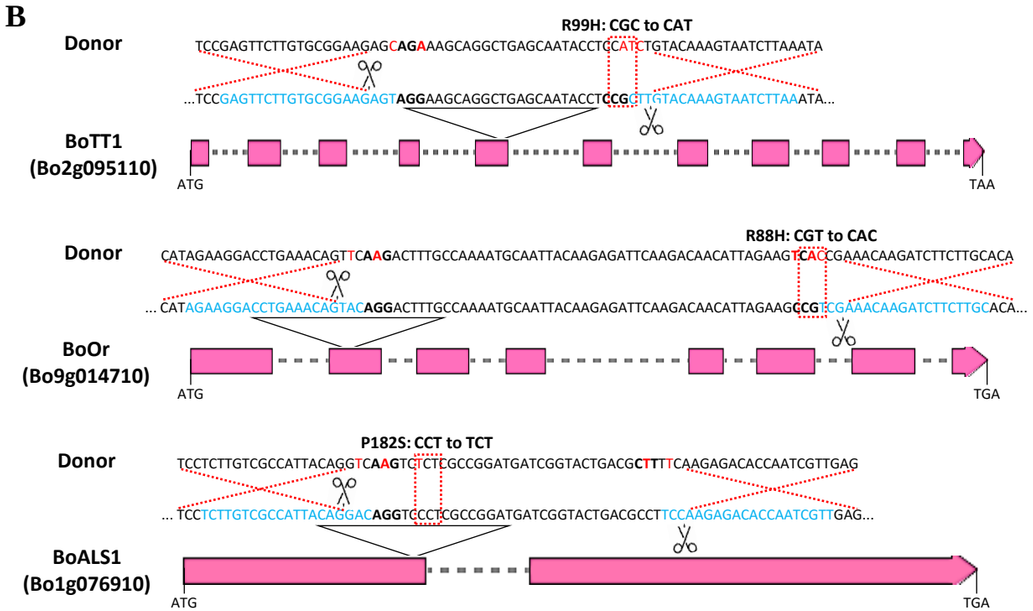

C

No.	Locus	Accession	Total reads	Targeted editing efficiency (%)	Precise editing efficiency (%)	gRNA1 indel rate (%)	gRNA2 indel rate (%)
1	LsTT1	XP_023737048	96871	0.78 ± 0.30	0.00	0.86 ± 0.71	0.35 ± 0.27
2	LsOr	XP_023743959	90601	0.42 ± 0.28	0.13 ± 0.10	1.07 ± 0.71	0.94 ± 0.39
3	LsALS1	XP_023747230	89394	4.47 ± 1.98	1.81 ± 0.75	2.69 ± 1.19	2.15 ± 0.99

D

No.	Locus	Accession	Total reads	Targeted editing efficiency (%)	Precise editing efficiency (%)	gRNA1 indel rate (%)	gRNA2 indel rate (%)
1	BoTT1	Bo2g095110	16905	8.98 ± 4.73	7.27 ± 4.46	4.83 ± 1.27	2.39 ± 1.20
2	BoOr	Bo9g014710	68028	2.95 ± 1.10	1.68 ± 0.24	24.37 ± 1.99	16.76 ± 6.12
3	BoALS1	Bo1g076910	90366	3.24 ± 1.54	0.73 ± 0.43	1.13 ± 0.49	10.61 ± 6.25

Figure 3. MMEJ-mediated precision gene editing in lettuce and cabbage.

(A-B) Schematic diagrams of targeted loci (TT1, Or, and ALS1 with their GenBank accession number), targeted sequences, gRNA binding sites, and MMEJ donors in lettuce (**A**) and cabbage (**B**). The targeted genes are shown from the start codon (ATG) to stop codons. Exons are drawn as colored boxes (purple boxes with lettuce's loci and pink boxes for cabbage), and the discontinuous line in each gene represents intron parts of the gene; the gRNA binding sequences are highlighted in light blue color with PAMs (bold nucleotides). The expected cutting sites (3-nt upstream of a PAM) are indicated with the black scissors; the intended base changes are painted in the red font; the targeted amino acid changes and corresponding triplexes are denoted by the discontinuous red boxes, and the texts placed on their top. The diagrams are not drawn to their scales.

(C) MMEJ-mediated editing efficiency in lettuce at the TT1, Or, and ALS1 loci.

(D) MMEJ-mediated editing efficiency in cabbage at the TT1, Or, and ALS1 loci.

SUPPLEMENTAL INFORMATION

Supplemental item	Page
Supplemental Figure 1. HR-independent strategies for precision gene/allele replacement using CRISPR/SpCas9	2
Supplemental Figure 2. Sanger sequencing data revealed precise replacement of DNA by MMEJ donor	3
Supplemental Figure 3. Indel alleles revealed from transfection of SpCas9, gR1.HPAT1 and gR2.HPAT3 with cNJ.HPAT3-1 donor	4
Supplemental Figure 4. Indel alleles revealed from transfection of SpCas9, gR1.HPAT1 and gR2.HPAT3 with MJ.HPAT3-1 donor	5
Supplemental Figure 5. Frequency of the MMEJ-mediated repaired products at different donor doses	6
Supplemental Figure 6. Identification of TT1, Or, and ALS1 genes in lettuce and cabbage for MMEJ-mediated gene targeting	7
Supplemental Table 1. gRNA, donor, and primer sequences employed in the study	8-10
Supplemental Table 2. cNHEJ- and MMEJ-mediated editing rates at SlHPAT3 locus revealed by Sanger sequencing	11
Supplemental Table 3. cNHEJ- and MMEJ-mediated editing rates of various repaired products at SlHPAT3 locus	12
Supplemental Table 4. Editing frequency of various repaired products revealed from treatments of different donor types and doses	13
Supplemental Table 5. MMEJ-mediated gene editing using various MJ.HPAT3-1 donor amounts (replicate)	14
Supplemental Table 6. MMEJ-mediated editing efficiency revealed from DSBs repair using donors with different microhomology lengths	15
Supplemental Table 7. Sequence alignment for selection of targeted genes in lettuce	16
Supplemental Table 8. Sequence alignment for selection of targeted genes in cabbage	17
Supplemental Table 9. Data revealed from the targeted deep-sequencing analysis of MMEJ-mediated editing in lettuce	18
Supplemental Table 10. Data revealed from the targeted deep-sequencing analysis of MMEJ-mediated editing in cabbage	19

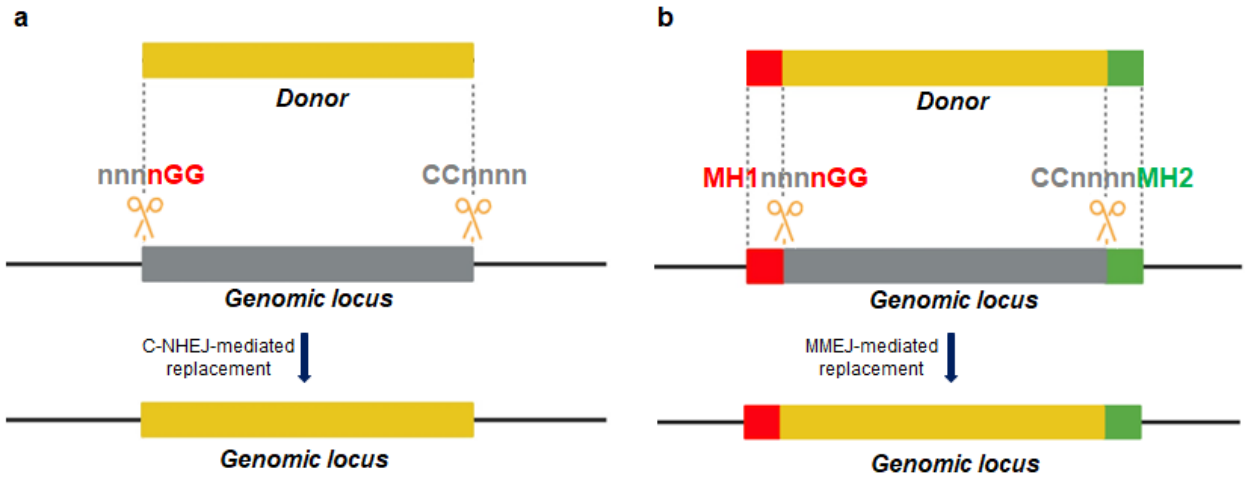

Supplemental Figure 1. HR-independent strategies for precision gene/allele replacement using CRISPR/SpCas9. (**a**) cNHEJ-mediated DNA replacement model. (**b**) MMEJ-mediated DNA replacement model. MH1 and MH2 are predefined from genomic loci and are subsequently introduced into the two ends of the donor sequence. CRISPR/Cas complexes are designed with canonical PAM binding sites (nGG/CCn) to produce DSBs at genomic loci with MH1 and MH2 flanking ends. MMEJ-mediated repair using the donor sequence generates genomic loci with precise modifications. The cut sites are arranged to avoid recurrent cutting. The orange sequences denote donors, and the gray indicates the genomic sequence being replaced. The letters n represent any nucleotide of A, T, G, or C except that the sequence-making gRNA spacers should not have more than 4 T in a row to avoid early transcription termination.

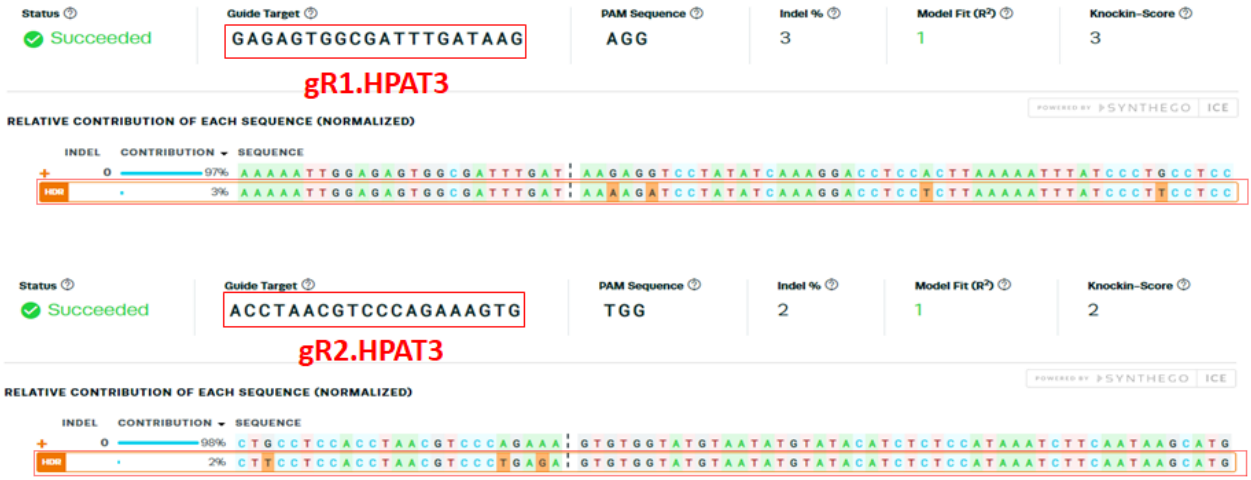

Supplemental Figure 2. Sanger sequencing data revealed precise replacement of DNA by MMEJ donor. PCR amplification of the targeted site was conducted using primers flanking the site and PCR products were resolved on gel and purified for Sanger sequencing. Sanger sequencing data were decomposed using the ICE Synthego web application using gR1.HPAT3 (upper panel) and gR2.HPAT3 (lower panel) for locating the cutting site. The edited allele and its percentage among the total sequence were revealed and highlighted in the discontinuous red boxes. The indented base changes of the left and right sides of the targeted sequence are highlighted in the orange background of the up and down panels, respectively.

Miniseq read	Product length	Read number	Edited type
gRNA1 ✂ gRNA2 ✂			
AGCTTGCTTACGGAAAAATTGGAGAGTGGCGATTTGATAAGAGGTCCTATATCAAAGGACCTCCACTTAAAAATTTATCCCTGCCTCCACCTAACGTCCCAGAAAGTGTGGTATGTAATATGTATACATC	130	30461	WT c
AGCTTGCTTACGGAAAAATTGGAGAGTGGCGATTTGAT----------AGTGTGGTATGTAATATGTATACATC	64	23884	del
AGCTTGCTTACGGAAAAATTGGAGAGTGGCGATTTGAT----------GTGTGGTATGTAATATGTATACATC	63	16471	del
AGCTTGCTTACGGAAAAATTGGAGAGTGGCG----------AGTGTGGTATGTAATATGTATACATC	57	2854	del
AGCTTGCTTACGGAAAAATTGGAGAGTGGCGAT----------AGTGTGGTATGTAATATGTATACATC	59	2619	del
AGCTTGCTTACGGAAAAATTGGAGAGTGGCGATTTG----------AGTGTGGTATGTAATATGTATACATC	62	2249	del
AGCTTGCTTACGGAAAAATTGGAGAGTGGCGATT----------GTGTGGTATGTAATATGTATACATC	59	1361	del
AGCTTGCTTACGGAAAAATTGGAGAGTGGCGATTT----------AGTGTGGTATGTAATATGTATACATC	61	1280	del
AGCTTGCTTACGGAAAAATTGGAGAGTGGCGAT----------GTGTGGTATGTAATATGTATACATC	58	1279	del
AGCTTGCTTACGGAAAAATTGGAGAGTGGCGATT----------AGTGTGGTATGTAATATGTATACATC	60	1229	del
AGCTTGCTTACGGAAAAATTGGAGAGTGGCG----------AAGTGTGGTATGTAATATGTATACATC	58	876	del
AGCTTGCTTACGGAAAAATTGGAGAGTGGCGATTTG----------AAGTGTGGTATGTAATATGTATACATC	63	850	del
AGCTTGCTTACGGAAAAATTGGAGAGTGGC----------GTGTGGTATGTAATATGTATACATC	55	632	del
AGCTTGCTTACGGAAAAATTGGAGAGTGGC----------AGTGTGGTATGTAATATGTATACATC	56	487	del
AGCTTGCTTACGGAAAAATTGGAGAGTGGCGATTTGATAAGAGGTCCTATATCAAAGGACCTCCACTTAAAAATTTATCCCTGCCTCCACCTAACGTCCCAGAAAAGTGTGGTATGTAATATGTATACATC	131	364	Ins
AGCTTGCTTACGGAAAAATTGGAGAGTGGC-----GATAAGAGGTCCTATATCAAAGGACCTCCACTTAAAAATTTATCCCTGCCTCCACCTAACGTCCCAGAAAGTGTGGTATGTAATATGTATACATC	125	354	del
AGCTTGCTTACGGAAAAATTGGAGAGTGGCGA----------TGTGGTATGTAATATGTATACATC	56	270	del
AGCTTGCTTACGGAAAAATTGGAGAGTGGCGAT----TAAGAGGTCCTATATCAAAGGACCTCCACTTAAAAATTTATCCCTGCCTCCACCTAACGTCCCAGAAAGTGTGGTATGTAATATGTATACATC	126	211	del
AGCTTGCTTACGGAAAAATTGGAGAGTGGCGATTTG----------GTGTGGTATGTAATATGTATACATC	61	200	del
AGCTTGCTTACGGAAAAATTGGAGAGTGGCGATTTGATTAAGAGGTCCTATATCAAAGGACCTCCACTTAAAAATTTATCCCTGCCTCCACCTAACGTCCCAGAAAGTGTGGTATGTAATATGTATACATC	131	200	Ins
AGCTTGCTTACGGAAAAATTGGAGAGTGGCGATTT----------GAAAGTGTGGTATGTAATATGTATACATC	64	148	del
AGCTTGCTTACGGAAAAATTGGAGAGTGGCGATTTGATAAGAGGTCCTATATCAAAGGACCTCCACTTAAAAATTTATCCCTGCCTCCACCTAACGTCCC----AGTGTGGTATGTAATATGTATACATC	126	129	del
AGCTTGCTTACGGAAAAATTGGAGAGTGGCGATTTGA----------TGTGGTATGTAATATGTATACATC	61	129	del
AGCTTGCTTACGGAAAAATTGGAGAG----------AGTGTGGTATGTAATATGTATACATC	52	117	del
AGCTTGCTTACGGAAAAATTGGAGAGTGGCGATTTGAT----------TGTGTGGTATGTAATATGTATACATC	64	114	del
AGCTTGCTTACGGAAAAATTGGAGAGTGGCGATT----------TGTGGTATGTAATATGTATACATC	58	113	del
AGCTTGCTTACGGAAAAATTGGAGAGTGGCGATT---TAAGAGGTCCTATATCAAAGGACCTCCACTTAAAAATTTATCCCTGCCTCCACCTAACGTCCCAGAAAGTGTGGTATGTAATATGTATACATC	127	107	del
AGCTTGCTTACGGAAAAATTGGAGAGTGGCGATTTGAT----------TGTGGTATGTAATATGTATACATC	62	105	del
AGCTTGCTTACGGAAAAATTGGAG----------AGTGTGGTATGTAATATGTATACATC	50	96	del
AGCTTGCTTACGGAAAAATTGG----------AGTGTGGTATGTAATATGTATACATC	48	92	del
AGCTTGCTTACGGAAAAATTGGAGAGTGGCGATTTG----------AGGTGTGGTATGTAATATGTATACATC	63	88	del
AGCTTGCTTACGGAAAAATTGGAGAGTGGCGATTTGATAAGAGGTCCTATATCAAAGGACCTCCACTTAAAAATTTATCCCTTCCTCCACCTAACGTCCCAGAAAGTGTGGTATGTAATATGTATACATC	130	88	WT c
AGCTTGCTTACGGAAAAATTGGAGAGTGGCGATTTGATAAGAGGTCCTATATCAAAGGACCTCCTCTTAAAAATTTATCCCTGCCTCCACCTAACGTCCCAGAAAGTGTGGTATGTAATATGTATACATC	130	84	WT c
GGCTTGCTTACGGAAAAATTGGAGAGTGGCGATTTGATAAGAGGTCCTATATCAAAGGACCTCCACTTAAAAATTTATCCCTGCCTCCACCTAACGTCCCAGAAAGTGTGGTATGTAATATGTATACATC	130	81	WT c
AGCTTGCTTACGGAAAAATTGGAGAGTGGCGATTTGATAAGAGGTCCTATATCAAAGGACCTCCACTTAAAAATTTATCCCTGCCTCCACCTAACGTCCCAG-AAGTGTGGTATGTAATATGTATACATC	129	75	del

Supplemental Figure 3. Indel alleles revealed from transfection of SpCas9, gR1.HPAT1 and gR2.HPAT3 with cNJ.HPAT3-1 donor. The gRNA binding and cutting sites are shown on the top panel with the scissor icons on the WT sequence.

Miniseq read	Product length	Read number	Edited type
gRNA1 ✂ gRNA2 ✂			
AGCTTGCTTACGGAAAAATTGGAGAGTGGCGATTTGATAAGAGGTCCTATATCAAAGGACCTCCACTTAAAAATTTATCCCTGCCTCCACCTAACGTCCCAGAAAGTGTGGTATGTAATATGTATACATC	130	44318	WT
AGCTTGCTTACGGAAAAATTGGAGAGTGGCGATTTGAT----------AGTGTGGTATGTAATATGTATACATC	64	17053	del
AGCTTGCTTACGGAAAAATTGGAGAGTGGCGATTTGAT----------GTGTGGTATGTAATATGTATACATC	63	11634	del
AGCTTGCTTACGGAAAAATTGGAGAGTGGCGAT----------AGTGTGGTATGTAATATGTATACATC	59	2190	del
AGCTTGCTTACGGAAAAATTGGAGAGTGGCG----------AGTGTGGTATGTAATATGTATACATC	57	2159	del
AGCTTGCTTACGGAAAAATTGGAGAGTGGCGATTTG----------AGTGTGGTATGTAATATGTATACATC	62	2060	del
AGCTTGCTTACGGAAAAATTGGAGAGTGGCGAT----------GTGTGGTATGTAATATGTATACATC	58	1317	del
AGCTTGCTTACGGAAAAATTGGAGAGTGGCGATT----------AGTGTGGTATGTAATATGTATACATC	60	1039	del
AGCTTGCTTACGGAAAAATTGGAGAGTGGCGATTT----------AGTGTGGTATGTAATATGTATACATC	61	909	del
AGCTTGCTTACGGAAAAATTGGAGAGTGGCG----------AAGTGTGGTATGTAATATGTATACATC	58	877	del
AGCTTGCTTACGGAAAAATTGGAGAGTGGCGATT----------GTGTGGTATGTAATATGTATACATC	59	813	del
AGCTTGCTTACGGAAAAATTGGAGAGTGGCGATTTGATAAAAGATCCTATATCAAAGGACCTCCACTTAAAAATTTATCCCTGCCTCCACCTAACGTCCCAGAAAGTGTGGTATGTAATATGTATACATC	130	722	WT
AGCTTGCTTACGGAAAAATTGGAGAGTGGCGATTT----------GTGTGGTATGTAATATGTATACATC	60	586	del
AGCTTGCTTACGGAAAAATTGGAGAGTGGCGATTTGATAAGAGGTCCTATATCAAAGGACCTCCTCTTAAAAATTTATCCCTGCCTCCACCTAACGTCCCAGAAAGTGTGGTATGTAATATGTATACATC	130	541	WT
AGCTTGCTTACGGAAAAATTGGAGAGTGGC----------AGTGTGGTATGTAATATGTATACATC	56	505	del
AGCTTGCTTACGGAAAAATTGGAGAGTGGCGATTTGATAAGAGGTCCTATATCAAAGGACCTCCACTTAAAAATTTATCCCTGCCTCCACCTAACGTCCCTGAGAGTGTGGTATGTAATATGTATACATC	130	429	WT
AGCTTGCTTACGGAAAAATTGGAGAGTGGCGATTTG----------AAGTGTGGTATGTAATATGTATACATC	63	414	del
AGCTTGCTTACGGAAAAATTGGAGAGTGGCGATTTGATAAGAGGTCCTATATCAAAGGACCTCCACTTAAAAATTTATCCCTTCCTCCACCTAACGTCCCTGAGAGTGTGGTATGTAATATGTATACATC	130	405	WT
AGCTTGCTTACGGAAAAATTGGAGAGTGGCGATTTGATAAGAGGTCCTATATCAAAGGACCTCCACTTAAAAATTTATCCCTGCCTCCACCTAACGTCCCAGAAAAGTGTGGTATGTAATATGTATACATC	131	396	Ins
AGCTTGCTTACGGAAAAATTGGAGAGTGGCGATTTGATAAGAGGTCCTATATCAAAGGACCTCCACTTAAAAATTTATCCCTTCCTCCACCTAACGTCCCAGAAAGTGTGGTATGTAATATGTATACATC	130	365	WT
AGCTTGCTTACGGAAAAATTGGAGAGTGGCG----------GTGTGGTATGTAATATGTATACATC	56	348	del
AGCTTGCTTACGGAAAAATTGGAGAGTGGC----------GTGTGGTATGTAATATGTATACATC	55	335	del
AGCTTGCTTACGGAAAAATTGGAGAGTGGCGATTTGATAAGAGGTCCTATATCAAAGGACCTCCTCTTAAAAATTTATCCCTTCCTCCACCTAACGTCCCTGAGAGTGTGGTATGTAATATGTATACATC	130	277	WT
AGCTTGCTTACGGAAAAATTGGAGAGTGGC-----GATAAGAGGTCCTATATCAAAGGACCTCCACTTAAAAATTTATCCCTGCCTCCACCTAACGTCCCAGAAAGTGTGGTATGTAATATGTATACATC	125	245	del
AGCTTGCTTACGGAAAAATTGGAGAGTGGCGATTTGATAAAAGATCCTATATCAAAGGACCTCCTCTTAAAAATTTATCCCTTCCTCCACCTAACGTCCCTGAGAGTGTGGTATGTAATATGTATACATC	130	220	WT
AGCTTGCTTACGGAAAAATTGGAGAGTGGCGATTTGATAAAAGATCCTATATCAAAGGACCTCCTCTTAAAAATTTATCCCTGCCTCCACCTAACGTCCCAGAAAGTGTGGTATGTAATATGTATACATC	130	197	WT
AGCTTGCTTACGGAAAAATTGGAGAGTGGCGATTTGATTAAGAGGTCCTATATCAAAGGACCTCCACTTAAAAATTTATCCCTGCCTCCACCTAACGTCCCAGAAAGTGTGGTATGTAATATGTATACATC	131	185	Ins
AGCTTGCTTACGGAAAAATTGGAGAGTGGCGATTTGAT----------TGTGGTATGTAATATGTATACATC	62	184	del
AGCTTGCTTACGG----------AAGTGTGGTATGTAATATGTATACATC	40	181	del
AGCTTGCTTACGGAAAAATTGGAGAGTGGCGATTTGATAAGAGGTCCTATATCAAAGGACCTCCTCTTAAAAATTTATCCCTTCCTCCACCTAACGTCCCAGAAAGTGTGGTATGTAATATGTATACATC	130	179	WT
AGCTTGCTTACGGAAAAATTGGAGAGTGGCGAT----TAAGAGGTCCTATATCAAAGGACCTCCACTTAAAAATTTATCCCTGCCTCCACCTAACGTCCCAGAAAGTGTGGTATGTAATATGTATACATC	126	178	del
AGCTTGCTTACGGAAAAATTGGAGAGTGGCGATTT----------GAAAGTGTGGTATGTAATATGTATACATC	64	170	del
AGCTTGCTTACGGAAAAATTGGAG----------AGTGTGGTATGTAATATGTATACATC	50	135	del
AGCTTGCTTACGGAAAAATTGGAGAGTGGCGATTTGATAAGAGGTCCTATATCAAAGGACCTCCACTTAAAAATTTATCCCTGCCTCCACCTAACGTCCC----AGTGTGGTATGTAATATGTATACATC	126	128	del
AGCTTGCTTACGGAAAAATTGGAGAGTGG----------AGTGTGGTATGTAATATGTATACATC	55	123	del

Supplemental Figure 4. Indel alleles revealed from transfection of SpCas9, gR1.HPAT1 and gR2.HPAT3 with MJ.HPAT3-1 donor. The gRNA binding and cutting sites are shown on the top panel with the scissor icons on the WT sequence.

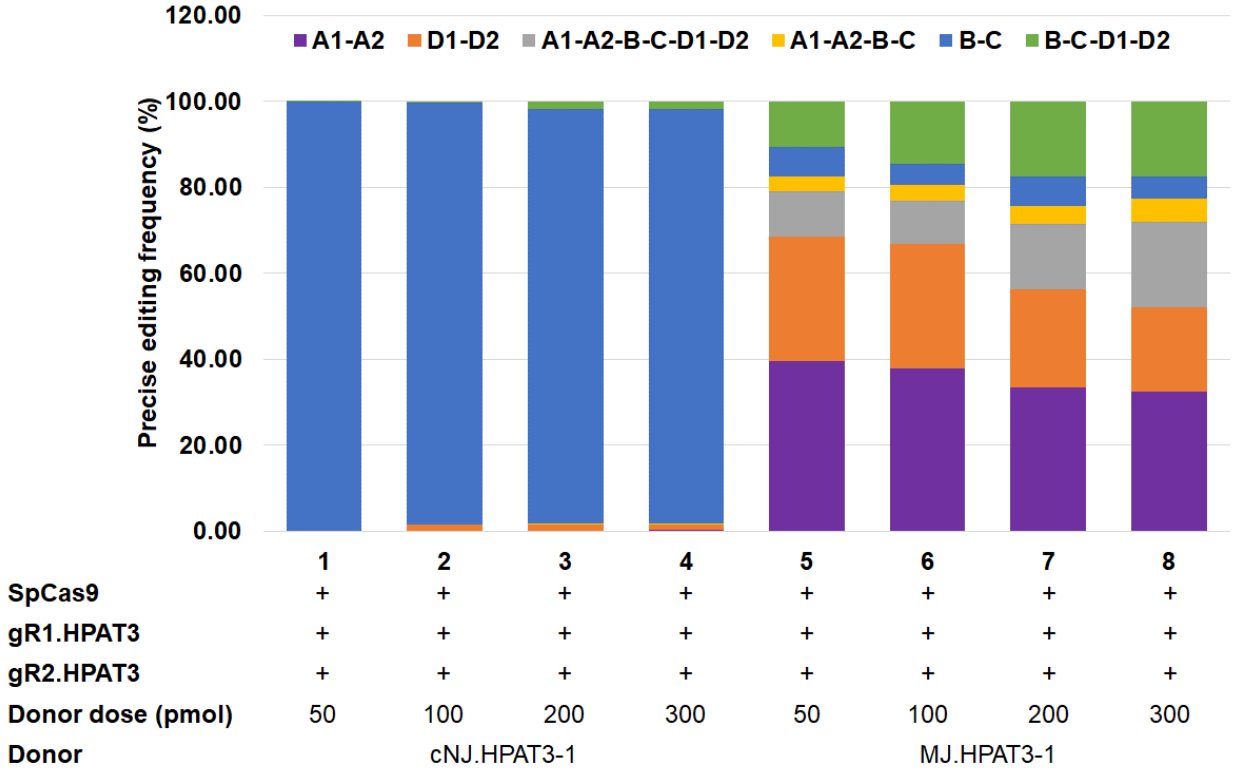

Supplemental Figure 5. The frequency of the MMEJ-mediated repaired products at different donor doses

Supplemental Figure 6. Identification of TT1, Or, and ALS1 genes in lettuce and cabbage for MMEJ-mediated gene targeting. **a**-**c**, Protein sequence alignment among tomato, lettuce, and cabbage for identification of targeted a.a changes in TT1 (**a**), Or (**b**), and ALS1 (b) genes. The targeted a.a is highlighted by the blue discontinuous boxes.

Supplemental Table 1. gRNA, donor, and primer sequences employed in the study

No.	Name	Sequence (5'-3')	Note
gRNA and donor sequences			
1	gR1.HPAT3	GAGAGTGGCGATTTGATAAG	gRNA1
2	gR2.HPAT3	ACCTAACGTCCCAGAAAGTG	gRNA2
3	gDR1.HPAT3	TTGATATAGGATCTTTTGCG	Donor gRNA1
4	gDR2.HPAT3	ACCTAACGTCCCTGAGAGCG	Donor gRNA2
5	gDR3.HPAT3	AAATCGCCACTCTCCAAGCG	Donor gRNA3
6	gDR4.HPAT3	TGGTATGTAATATGTATGCG	Donor gRNA4
7	cNJ.HPAT3-1	AAAAGATCCTATATCAAAGGACCTCCTCTTAAAAATTTATCCCTTCCTCCACCTAACGTCCCTGAGA	cNJ.HPAT3-1 donor
8	MJ.HPAT3-1	TTGGAGAGTGGCGATTTGATAAAAGATCCTATATCAAAGGACCTCCTCTTAAAAATTTATCCCTTCCTCCACCTAACGTCCCTGAGAGTGTGGTATGTAATATGTAT	MJ.HPAT3-1 donor
9	MJ.HPAT3-2	GCGATTTGATAAAAGATCCTATATCAAAGGACCTCCTCTTAAAAATTTATCCCTTCCTCCACCTAACGTCCCTGAGAGTGTGGTATG	MJ.HPAT3-2 donor
10	MJ.HPAT3-3	TTGATAAAAGATCCTATATCAAAGGACCTCCTCTTAAAAATTTATCCCTTCCTCCACCTAACGTCCCTGAGAGTGTG	MJ.HPAT3-3 donor
11	gR1.LsTT1	GAGTTCTAGTCAGGAAGAGC	gRNA1
12	gR2.LsTT1	ACAGCCCTAAAAGTGTGAAT	gRNA2
13	MJ.LsTT1	CTAGAGTTCTAGTCAGGAAGAGTAGAAAGCAAGCAGAACAATACCATCATCTATACAAAGTACGCTTATTGTCCAACTCACACTTTTAGGGCTGTTTCT	MJ.LsTT1 donor
14	gR1.LsOr	AAGATAATATTAGAAGTCGT	gRNA1
15	gR2.LsOr	GAGGAGGTGAGCAAGTTTTT	gRNA2
16	MJ.LsOr	TTCAAGATAATATTAGAAGTCATAGAAATAAAATATTTTTACACATGGAGGAGGTGAGCAAATCTTTCGGAATATTCATCTGTA	MJ.LsOr donor
17	gR1.LsALS1	CCATCACCGGCCAAGTCCCC	gRNA1
18	gR2.LsALS1	ACGCGTTACCTCCACAATCG	gRNA2
19	MJ.LsALS1	TTGCCATCACCGGCCAAGTCTCTCGTAGAATGATCGGAACCGATGCGTTTCAAGAAACTCCAATTGTGGAGGTAACGCGTTCC	MJ.LsALS1 donor
20	gR1.BoTT1	GAGTTCTTGTGCGGAAGAGT	gRNA1
21	gR2.BoTT1	TTAAGATTACTTTGTACAAG	gRNA2
22	MJ.BoTT1	TCCGAGTTCTTGTGCGGAAGAGCAGAAAGCAGGCTGAGCAATACCTCCATCTGTACAAAGTAATCTTAAATA	MJ.BoTT1 donor
23	gR1.BoOr	AGAAGGACCTGAAACAGTAC	gRNA1
24	gR2.BoOr	GCAAGAAGATCTTGTTTCGA	gRNA2
25	MJ.BoOr	CATAGAAGGACCTGAAACAGTTCAAGACTTTGCCAAAATGCAATTACAAGAGATTCAAGACAACATTAGAAGTCACCGAAACAAGATCTTCTTGCACA	MJ.BoOr donor
26	gR1.BoALS1	TCTTGTCGCCATTACAGGAC	gRNA1
27	gR2.BoALS1	AACGATTGGTGTCTCTTGGA	gRNA2
28	MJ.BoALS1	TCCTCTTGTCGCCATTACAGGTCAAGTCTCTCGCCGGATGATCGGTACTGACGCTTTTCAAGAGACACCAATCGTTGAG	MJ.BoALS1 donor
Primers for donor preparation			
29	cNJ.HPAT-F1	AAAAGATCCTATATCAAAGGACCTCCTCTTAAAAATTTATCCCT	

30	cNJ.HPAT-R1	TCTCAGGGACGTTAGGTGGAGGAAGGGATAAATTTTTAAGAGGAGG	Primers for preparing cNJ.HPAT3.1 donor. The phosphodiester linkages between the red nucleotides were modified with phosphorothioate bond
31	MJ.HPAT-F1	TTGGAGAGTGGCGATTTGATAAAAGATCCTATATCAAAGGACCTCCTCTTAAAAATTTATCCCT	Primers for preparing MJ.HPAT3.1 donor
32	MJ.HPAT-R1	ATACATATTACATACCACACTCTCAGGGACGTTAGGTGGAGGAAGGGATAAATTTTTAAGAGGAGG	
33	MJ.HPAT-F2	GCGATTTGATAAAAGATCCTATATCAAAGGACCTCCTCTTAAAAATTTATCCCT	Primers for preparing MJ.HPAT3.2 donor
34	MJ.HPAT-R2	CATACCACACTCTCAGGGACGTTAGGTGGAGGAAGGGATAAATTTTTAAGAGGAGG	
35	MJ.HPAT-F3	TTGATAAAAGATCCTATATCAAAGGACCTCCTCTTAAAAATTTATCCCT	Primers for preparing MJ.HPAT3.3 donor
36	MJ.HPAT-R3	CACACTCTCAGGGACGTTAGGTGGAGGAAGGGATAAATTTTTAAGAGGAGG	
37	MJ.BoTT1-F1	TCCGAGTTCTTGTGCGGAAGAGCAGAAAGCAGGCTGAGCAATACCTCC	Primers for preparing MJ.BoTT1 donor
38	MJ.BoTT1-R1	TATTTAAGATTACTTTGTACAGATGGAGGTATTGCTCAGCCTGCTTTC	
39	MJ.LsTT1-F1	CTAGAGTTCTAGTCAGGAAGAGTAGAAAGCAAGCAGAACAATACCATCATCTATACAAAGTACGC	Primers for preparing MJ.LsTT1 donor
40	MJ.LsTT1-R1	AGAAACAGCCCTAAAAGTGTGAGTTGGACAATAAGCGTACTTTGTATAGATGATGGTATTGT	
41	MJ.BoOr-F1	CATAGAAGGACCTGAAACAGTTCAAGACTTTGCCAAAATGCAATTACAAGAGATTCAAGACA	Primers for preparing MJ.BoOr donor
42	MJ.BoOr-R1	TGTGCAAGAAGATCTTGTTTCGGTGACTTCTAATGTTGTCTTGAATCTCTTGTAATTGCATT	
43	MJ.LsOr-F1	TTCAAGATAATATTAGAAGTCATAGAAATAAAATATTTTTACACATGGAGGAGGTG	Primers for preparing MJ.LsOr donor
44	MJ.LsOr-R1	TACAGATGAATATTCCGAAAGATTTGCTCACCTCCTCCATGTGTAAAAATATTT	
45	MJ.BoALS1-F1	TCCTCTTGTCGCCATTACAGGTCAAGTCTCTCGCCGGATGATCGGTACTGAC	Primers for preparing MJ.BoALS1 donor
46	MJ.BoALS1-R1	CTCAACGATTGGTGTCTCTTGAAAAGCGTCAGTACCGATCATCCGGCGAGAG	
47	MJ.LsALS1-F1	TTGCCATCACCGGCCAAGTCTCTCGTAGAATGATCGGAACCGATGCGTTTCAAG	Primers for preparing MJ.LsALS1 donor
48	MJ.LsALS1-R1	GGAACGCGTTACCTCCACAATTGGAGTTTCTTGAAACGCATCGGTTCCGATCATT	
Primers for miniseq sample preparation			
49	BoTT1-F1	GCTCCTTTGCTCACTTAGATCA	First PCR
50	BoTT1-R1	GCAAATTGTGTATTGAAGTGAATTATGATC	
51	BoTT1-F2	ACACTCTTTCCCTACACGACGCTCTTCCGATCTGCTTCTCTGTAGTGGTATGGGCCC	Second PCR

52	BoTT1-R2	GTGACTGGAGTTCAGACGTGTGCTCTTCCGATCTACAATACTCC AAGAAAAGTAGATGAG	
53	BoOr-F1	GTTCGTAATAGAGTGTGGTGGT	First PCR
54	BoOr-R1	AGAGGATAATCCCAGCAATGAG	
55	BoOr-F2	ACACTCTTTCCCTACACGACGCTCTTCCGATCTTGATTATTTTTGG TGCAGCTTTTGTATC	Second PCR
56	BoOr-R2	GTGACTGGAGTTCAGACGTGTGCTCTTCCGATCTCCACTTTAAG AAAGTAAACCTCTTCC	
57	BoALS1-F1	CCCTCTACCCATTTCCAGATTC	First PCR
58	BoALS1-R1	CTATGCTCCACAGCGTAGTTAG	
59	BoALS1-F2	ACACTCTTTCCCTACACGACGCTCTTCCGATCTGTTAGCAGACGC GATGCTTGACA	Second PCR
60	BoALS1-R2	GTGACTGGAGTTCAGACGTGTGCTCTTCCGATCTGGTATGTCAT CAACATCCATCACCAA	
61	LsTT1-F1	TCAGATTGAACATGCCCTCAC	First PCR
62	LsTT1-R1	GCCTTACACCACTACACAAAGA	
63	LsTT1-F2	ACACTCTTTCCCTACACGACGCTCTTCCGATCTTCATTTCCAGTGG CATGGGGCC	Second PCR
64	LsTT1-R2	GTGACTGGAGTTCAGACGTGTGCTCTTCCGATCTGTCCAAATTA AGTGCTTAACCCATTAAG	
65	LsOr-F1	AAGGAGGGCGACTGATAATTG	First PCR
66	LsOr-R1	CTTACTGTAGGTGCAAGGAGAC	
67	LsOr-F2	ACACTCTTTCCCTACACGACGCTCTTCCGATCTAACAGTCCAGGA CTTTGATAAAATGG	Second PCR
68	LsOr-R2	GTGACTGGAGTTCAGACGTGTGCTCTTCCGATCTGCATAACGCA ATTAGATAACTCACGC	
69	LsALS1-F1	CCTTCTATCACCCACCCATTTC	First PCR
70	LsALS1-R1	TCCGAGCATTTGAAGGGATAAA	
71	LsALS1-F2	ACACTCTTTCCCTACACGACGCTCTTCCGATCTACGCGCTGCTCG ACAGTATCCC	Second PCR
72	LsALS1-R2	GTGACTGGAGTTCAGACGTGTGCTCTTCCGATCTACATCCAAAA CAAGGTAATTGTGTTTAG	
Primers for Sanger sequencing			
73	HPAT3-sF1	CACCTTGGGATTTGGACAGTAG	SlHPAT3

Supplemental Table 2. cNHEJ- and MMEJ-mediated editing rates at SlHPAT3 locus revealed by Sanger sequencing

Treatment	SpCas9	gR1.HPAT3	gR2.HPAT3	Donor	Precise editing efficiency* (%)	Targeted editing efficiency** (%)
1	-	-	-	-	0.0	0.0
2	+	+	-	-	0.0	0.0
3	+	-	+	-	0.0	0.0
4	+	+	+	-	0.0	0.0
5	+	+	+	cNHEJ.HPAT3-1	0.0	1.0
6	+	+	+	MMEJ.HPAT3-1	2.0	3.0

** Precise editing efficiency was calculated by dividing total reads containing all the base changes by the total reads.*
***Targeted-editing efficiency is the portion of the precisely edited products containing all the base changes and those containing only B and C base changes among all the edited products.*

Supplemental Table 3. cNHEJ- and MMEJ-mediated editing rates of various repaired products at SlHPAT3 locus

Edited SNPs	Donor			
	cNJ.HPAT3-1		MJ.HPAT3-1	
	Number of edited reads	Relative editing frequency (%)	Number of edited reads	Relative editing frequency (%)
A1-A2-B-C-D1-D2	0	0.00	237	9.72
A1-A2	0	0.00	872	35.77
A1-A2-B-C	0	0.00	150	6.15
B-C	72	94.74	169	6.93
B-C-D1-D2	4	5.26	249	10.21
D1-D2	0	0.00	761	31.21
Number of edited reads	76	100.000	2438	100.00
Total reads	93054	-	99885	-

Supplemental Table 4. Editing frequency of various repaired products revealed from treatments of different donor types and doses

Edited alleles	Mock		cNJ.HPAT3.1 donor amount (pmol)								MJ.HPAT3.1 donor amount (pmol)							
	0		50		100		200		300		50		100		200		300	
	Number of reads	Frequency (%)	Number of reads	Frequency (%)	Number of reads	Frequency (%)	Number of reads	Frequency (%)	Number of reads	Frequency (%)	Number of reads	Frequency (%)	Number of reads	Frequency (%)	Number of reads	Frequency (%)	Number of reads	Frequency (%)
A1-A2	0	0.00	0	0.00	0	0.00	0	0.00	2	0.42	719	39.66	699	37.85	522	33.42	461	32.56
D1-D2	0	0.00	1	0.17	8	1.48	8	1.43	5	1.05	525	28.96	534	28.91	358	22.92	278	19.63
A1-A2-B-C-D1-D2	0	0.00	0	0.00	0	0.00	1	0.18	0	0.00	189	10.42	185	10.02	238	15.24	281	19.84
A1-A2-B-C	0	0.00	0	0.00	0	0.00	1	0.18	1	0.21	65	3.59	68	3.68	65	4.16	75	5.30
B-C	0	0.00	601	99.67	533	98.34	541	96.43	459	96.63	122	6.73	94	5.09	107	6.85	72	5.08
B-C-D1-D2	0	0.00	1	0.17	1	0.18	10	1.78	8	1.68	193	10.65	267	14.46	272	17.41	249	17.58
Total reads with edited bases	**0**	0.000	**603**	100.00	**542**	100.00	**561**	100.00	**475**	100.00	**1813**	100.00	**1847**	100.00	**1562**	100.00	**1416**	100.00
Total read	**27391**	**-**	**31995**	-	**36917**	-	**33600**	-	**27420**	-	**29937**	-	**27998**	-	**28611**	-	**28296**	-
Total editing efficiency (%)*	**0.00**		**1.88**		**1.47**		**1.67**		**1.73**		**6.06**		**6.60**		**5.46**		**5.00**	
Targeted editing ratio (%)**	**0.00**		**99.83**		**98.52**		**98.57**		**98.53**		**31.38**		**33.24**		**43.66**		**47.81**	

** Total editing efficiency is a sum of all the MMEJ-mediated editing efficiency ((Total reads with edited bases/Total read) x 100).*

*** Targeted-editing ratio is the portion of the precisely edited products containing all the base changes and those containing only B and C base changes among all the edited products.*

Supplemental Table 5. MMEJ-mediated gene editing using various MJ.HPAT3-1 donor amounts (replicate)

Treatment	Donor amount (pmol)	Total reads	Precise editing efficiency* (%)	Only B and C editing efficiency (%)**	gRNA1 indel rate (%)	gRNA2 indel rate (%)
1	300	23848	0.105	0.587	3.329	3.350
2	200	29643	0.078	0.523	3.077	3.080
3	100	26579	0.090	0.764	3.525	3.424
4	50	25108	0.008	0.119	2.880	2.824

** Precise editing efficiency was calculated by dividing total reads containing all the base changes by the total reads.*

*** The only B and C editing efficiency were calculated by dividing total reads containing the only B and C base changes by the total reads*

Supplemental Table 6. MMEJ-mediated editing efficiency revealed from DSBs repair using donors with different microhomology lengths.

Donor	Replicate	Total reads	Total editing efficiency (%)**	Targeted editing efficiency (%)	Precise editing efficiency (%)	Only B and C editing efficiency (%)	One-sided editing efficiency (%)	gRNA1 indel rate (%)	gRNA2 indel rate (%)
-	1	76598	0.00	0.00	0.00	0.00	0.00	0.62	0.62
-	2	76002	0.00	0.00	0.00	0.00	0.00	1.39	1.36
Average		-	0.00	0.00	0.00	0.00	0.00	1.01	0.99
SEM		-	0.00	0.00	0.00	0.00	0.00	0.38	0.37
MJ.HPAT3-1	1	74776	4.62	1.12	0.32	0.80	3.50	0.73	0.73
MJ.HPAT3-1	2	72689	5.32	1.40	0.40	1.00	3.92	0.69	0.68
MJ.HPAT3-1	3	28491	3.80	1.12	0.21	0.92	2.67	2.23	2.18
MJ.HPAT3-1	4	20879	3.16	1.01	0.19	0.81	2.16	4.26	4.26
Average		-	4.22	1.16	0.28	0.88	3.06	1.98	1.96
SEM		-	0.47	0.09	0.05	0.05	0.40	0.84	0.84
p (MJ.HPAT3-1 vs MJ.HPAT3-2)*		-	0.0064	0.0007	0.0025	0.0024	0.0016	0.9310	0.9419
p (MJ.HPAT3-1 vs MJ.HPAT3-3)		-	0.0179	0.0002	<0.0001	0.0015	<0.0001	0.5456	0.5619
MJ.HPAT3-2	1	75083	1.76	0.42	0.10	0.32	1.34	0.18	0.19
MJ.HPAT3-2	2	67743	3.01	0.76	0.19	0.57	2.25	0.34	0.40
MJ.HPAT3-2	3	25992	2.72	0.94	0.15	0.79	1.92	4.21	4.19
MJ.HPAT3-2	4	28214	1.85	0.52	0.06	0.46	1.33	2.71	2.68
Average		-	2.33	0.66	0.12	0.54	1.71	1.86	1.86
SEM		-	0.31	0.12	0.03	0.10	0.23	0.97	0.96
p (MJ.HPAT3-2 vs MJ.HPAT3-3)		-	0.5903	0.3657	0.0731	0.7876	0.0654	0.6539	0.6544
MJ.HPAT3-3	1	65392	1.91	0.62	0.06	0.56	1.29	0.39	0.38
MJ.HPAT3-3	2	68109	1.44	0.41	0.06	0.35	1.03	0.32	0.35
MJ.HPAT3-3	3	28571	3.37	0.49	0.02	0.47	0.72	2.50	2.47
MJ.HPAT3-3	4	26584	3.89	0.70	0.04	0.66	1.09	2.09	2.14
Average		-	2.65	0.55	0.04	0.51	1.03	1.32	1.33
SEM		-	0.58	0.06	0.01	0.07	0.12	0.57	0.57

**p-value returned from Uncorrected Fisher's LSD test. ** Total editing efficiency is the sum of all the MMEJ-mediated editing efficiency without considering the indel mutation efficiency of the gRNAs. Targeted editing efficiency is the sum of the precise editing efficiency and the only B and C editing efficiency. Precise editing efficiency was calculated by dividing total reads containing all the base changes by the total reads. The only B and C editing efficiency were calculated by dividing total reads containing the only B and C base changes by the total reads. One-sided editing efficiency was calculated by dividing total reads containing either the left-sided bases (A1 and A2) or the right-sided base pairs (D1 and D2) by the total reads*

Supplemental Table 7. Sequence alignment for selection of targeted genes in lettuce

Gene ID	Identity (%)	Alignment length (a.a)	E-value	Bitscore
TT1				
XP_023737048.1	93.617	235	3.60E-164	453
XP_023733423.1	38.767	227	1.51E-50	165
XP_023758433.1	35.526	228	5.80E-47	156
XP_023734413.1	36.325	234	2.22E-46	154
XP_023770770.1	35.043	234	2.55E-45	152
Orange				
XP_023743959.1	85.657	462	3.03E-165	453
PLY66076.1	85.657	462	3.22E-163	165
XP_023734734.1	68.775	362	1.56E-125	156
ALS1				
XP_023747230.1	83.043	659	0	1068
PLY79534.1	61.836	249	1.14E-82	262
PLY79513.1	65.574	652	5.42E-52	176
XP_023754650.1	25.664	630	3.49E-40	155
XP_023750264.1	23.897	578	1.03E-15	81.3

Supplemental Table 8. Sequence alignment for selection of targeted genes in cabbage

Gene ID	Identity (%)	Alignment Length (a.a)	E-value	Bitscore
TT1				
Bo2g095110	94.1	236	7.4e-120	433.0
Bo6g081130	93.6	236	1.6e-119	431.8
Bo6g123660	93.2	236	1.6e-119	431.8
Or				
Bo9g014710	74.4	312	2.0e-104	382.1
Bo2g007140	68.3	249	3.3e-75	285.0
ALS1				
Bo1g076910	74.4	666	6.0e-244	846.7
Bo7g082530	68.3	638	4.6e-143	511.5

Supplemental Table 9. Data revealed from the targeted deep-sequencing analysis of MMEJ-mediated editing in lettuce

No.	Targeted gene	Replicate	Total reads	Total editing efficiency (%)*	Targeted editing efficiency (%)**	Precise editing efficiency (%)***	Desirable base change efficiency (%)****	One-sided editing efficiency (%)*****	gRNA1 indel rate (%)	gRNA2 indel rate (%)
1	LsTT1	1	31767	2.62	0.81	0.00	0.81	1.81	2.26	0.88
2	LsTT1	2	33468	4.44	1.29	0.00	1.29	3.15	0.31	0.13
3	LsTT1	3	31636	0.82	0.26	0.00	0.26	0.56	0.02	0.03
Average			**96871**	**2.63**	**0.78**	**0.00**	**0.78**	**1.84**	**0.86**	**0.35**
SEM******			590	1.05	0.30	0.00	0.30	0.75	0.71	0.27
4	LsOr	1	29362	0.48	0.09	0.02	0.07	0.39	2.48	1.73
5	LsOr	2	29362	0.82	0.20	0.04	0.15	0.62	0.32	0.50
6	LsOr	3	31877	3.94	0.97	0.33	0.64	2.97	0.40	0.60
Average			**90601**	**1.74**	**0.42**	**0.13**	**0.29**	**1.33**	**1.07**	**0.94**
SEM			838.33	1.10	0.28	0.10	0.18	0.82	0.71	0.39
7	LsALS1	1	25553	2.74	1.53	0.44	1.09	1.22	0.97	0.41
8	LsALS1	2	26629	13.62	8.23	3.03	5.19	5.39	2.13	2.20
9	LsALS1	3	37212	5.37	3.65	1.96	1.68	1.72	4.96	3.83
Average			**89394**	**7.24**	**4.47**	**1.81**	**2.66**	**2.78**	**2.68**	**2.15**
SEM			3720	3.28	1.98	0.75	1.28	1.31	1.19	0.99

** Total editing efficiency is a sum of all the MMEJ-mediated editing efficiency without considering the indel mutation efficiency of the gRNAs. ** Targeted editing efficiency is the sum of the precise editing efficiency and the desirable base change efficiency. ***Precise editing efficiency was calculated by dividing total reads containing all the base changes by the total reads. ****The desirable base change efficiency was calculated by dividing total reads containing only the targeted a.a changes by the total reads. *****One-sided editing efficiency was calculated by dividing total edited reads not containing targeted a.a change by the total reads. ******SEM: Standard error of the mean.*

Supplemental Table 10. Data revealed from the targeted deep-sequencing analysis of MMEJ-mediated editing in cabbage

No.	Targeted gene	Replicate	Total reads	Total editing efficiency (%)*	Targeted editing efficiency (%)**	Precise editing efficiency (%)***	Desirable base change efficiency (%)****	One-sided editing efficiency (%)*****	gRNA1 indel rate (%)	gRNA2 indel rate (%)
1	BoTT1	1	6647	1.64	1.37	0.57	0.8	0.27	2.72	0.56
2	BoTT1	2	3719	20.25	17.64	15.73	1.91	2.61	7.13	4.65
3	BoTT1	3	6539	10.25	7.94	5.51	2.43	2.31	4.65	1.97
Average			**16905**	**10.71**	**8.98**	**7.27**	**1.71**	**1.73**	**4.83**	**2.39**
SEM******			-	5.38	4.73	4.46	0.48	0.73	1.27	1.2
4	BoOr	1	17556	2.49	1.95	1.38	0.57	0.54	21.94	9.27
5	BoOr	2	28622	5.69	3.95	1.98	1.97	1.75	26.8	24.26
6	BoOr	3	21850	0.28	0.14	0.01	0.13	0.14	11.73	6.58
Average			**68028**	**4.09**	**2.95**	**1.68**	**1.27**	**1.15**	**24.37**	**16.76**
SEM			-	1.31	1.10	0.24	0.57	0.49	1.99	6.12
7	BoALS1	1	30301	0.38	0.22	0.04	0.18	0.16	0.43	6.7
8	BoALS1	2	38778	7.93	5.32	1.19	4.13	2.61	1.16	4.39
9	BoALS1	3	21287	6.2	4.17	0.96	3.21	2.02	1.81	20.74
Average			**90366**	**4.84**	**3.24**	**0.73**	**2.51**	**1.6**	**1.13**	**10.61**
SEM			-	2.8	1.54	0.43	1.46	0.9	0.49	6.25

** Total editing efficiency is a sum of all the MMEJ-mediated editing efficiency without considering the indel mutation efficiency of the gRNAs. ** Targeted editing efficiency is the sum of the precise editing efficiency and the desirable base change efficiency. ***Precise editing efficiency was calculated by dividing total reads containing all the base changes by the total reads. ****The desirable base change efficiency was calculated by dividing total reads containing only the targeted a.a changes by the total reads. *****One-sided editing efficiency was calculated by dividing total edited reads not containing targeted a.a change by the total reads. ******SEM: Standard error of the mean.*

SEQUENCES USED IN THE STUDY

- **SlHPAT3 cNHEJ donor (cNJ.HPAT3-1)**

  5'-AAaAGaTCCTATATCAAAGGACCTCCtCTTAAAAATTTATCCCTtCCTCCACCTAACGTCCCtGAgA-3'

  Blue font: introduced bases. From 5'-3': the bases were named A1; A2; B; C; D1; D2, respectively.

- **SlHPAT3 MMEJ donor (MJ.HPAT3-1)**

  5'-ATTGGAGAGTGGCGATTTGATAAaAGaTCCTATATCAAAGGACCTCCtCTTAAAAATTTATCCCTtCCTCCACCTAACGTCCCtGAgAGTGTGGTATGTAATATGTAT-3'

  black font: replaced sequence; Blue font: introduced bases. From 5'-3': the bases were named A1; A2; B; C; D1; D2, respectively; red font: MH1; green font: MH2.

- **SlHPAT3 MMEJ donor (MJ.HPAT3-2)**

  5'-GGCGATTTGATAAaAGaTCCTATATCAAAGGACCTCCtCTTAAAAATTTATCCCTtCCTCCACCTAACGTCCCtGAgAGTGTGGTATG-3'

  black font: replaced sequence; Blue font: introduced bases. From 5'-3': the bases were named A1; A2; B; C; D1; D2, respectively; red font: MH1; green font: MH2.

- **SlHPAT3 MMEJ donor (MJ.HPAT3-3)**

  5'-TTGATAAaAGaTCCTATATCAAAGGACCTCCtCTTAAAAATTTATCCCTtCCTCCACCTAACGTCCCtGAgAGTGTG-3'

  black font: replaced sequence; Blue font: introduced bases. From 5'-3': the bases were named A1; A2; B; C; D1; D2, respectively; red font: MH1; green font: MH2.

- **LsTT1 MMEJ donor**

  CTAGAGTTCTAGTCAGGAAGAGtAGaAAGCAAGCAGAACAATACCATCatCTATACAAAGTACGCTTATTGTCCaAcTCACACTTTTAGGGCTGTTTCT

  Blue font: introduced bases; red font: MH1; green font: MH2.

- **LsOR MMEJ donor**

TTCAAGATAATATTAGAAGTCaTaGaAATAAAATATTTTTACACATGGAGGAGGTGAGCAAaTcTTTC
GGAATATTCATCTGTA

Blue font: introduced bases; red font: MH1; green font: MH2.

- **LsALS1 MMEJ donor**

TTGCCATCACCGGCCAAGTCtCtCGtAGAATGATCGGAACCGATGCGTTTCAAGAAACtCCaATTGTG
GAGGTAACGCGTTCC

Blue font: introduced bases; red font: MH1; green font: MH2.

- **BoTT1 MMEJ donor**

TCCGAGTTCTTGTGCGGAAGAGcAGaAAGCAGGCTGAGCAATACCTCCatcTGTACAAAGTAATCTTAA
ATA

Blue font: introduced bases.

- **BoOR MMEJ donor**

CATAGAAGGACCTGAAACAGTtCAaGACTTTGCCAAAATGCAATTACAAGAGATTCAAGACAACATTA
GAAGtCacCGAAACAAGATCTTCTTGCACA

Blue font: introduced bases; red font: MH1; green font: MH2.

- **BoALS1 MMEJ donor**

TCCTCTTGTCGCCATTACAGGtCAaGTCtCTCGCCGGATGATCGGTACTGACGCtTTtCAAGAGACACCA
ATCGTTGAG

Blue font: introduced bases; red font: MH1; green font: MH2.